CHALMERS
UNIVERSITY OF TECHNOLOGY

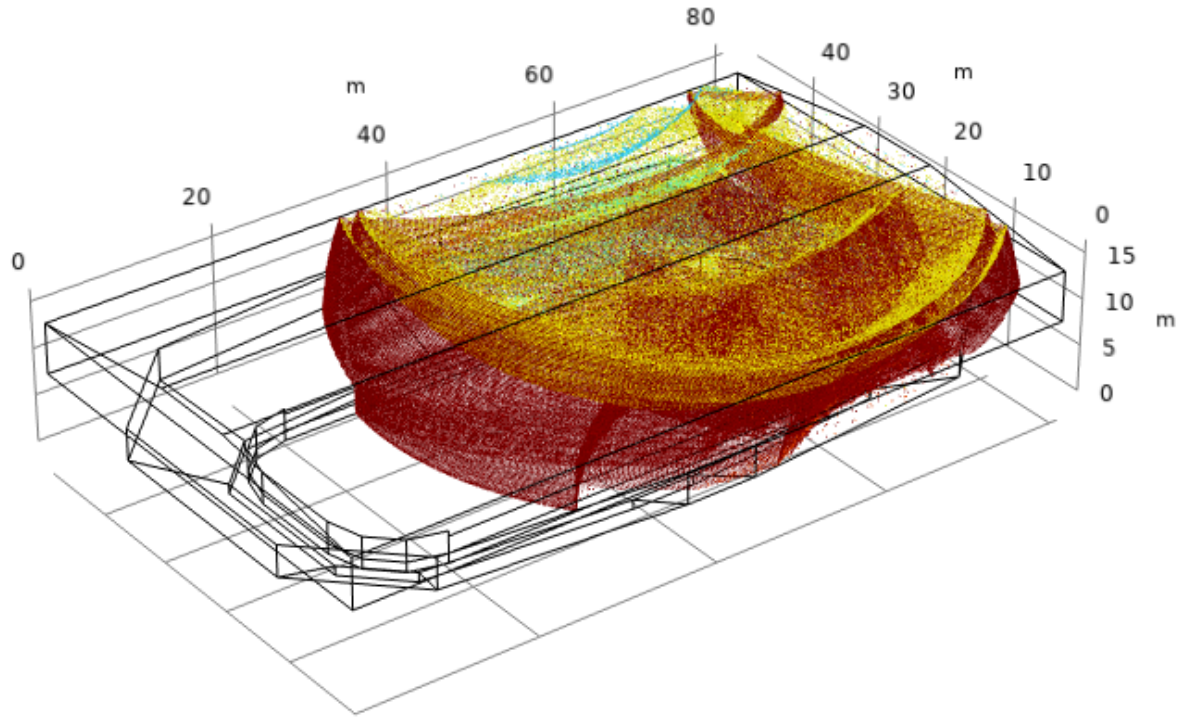

Influence of Temperature Gradients on the Sound Field in Ice Hockey Halls

Master's thesis in Sound and Vibration

ALEXANDRA PAPPA

DEPARTMENT OF ARCHITECTURE AND CIVIL ENGINEERING

CHALMERS UNIVERSITY OF TECHNOLOGY
Gothenburg, Sweden 2024
www.chalmers.se

Master's thesis 2024

Influence of Temperature Gradients on the Sound Field in Ice Hockey Halls

ALEXANDRA PAPPA

CHALMERS
UNIVERSITY OF TECHNOLOGY

Department of Architecture and Civil Engineering
Division of Applied Acoustics
Chalmers University of Technology
Gothenburg, Sweden 2024

Influence of Temperature Gradients on the Sound Field in Ice Hockey Halls
ALEXANDRA PAPPA

Supervisor: Jorge Torres, Brekke & Strand Akustikk AS
Examiner: Wolfgang Kropp, Division of Applied Acoustics, Chalmers University of Technology

Master's Thesis 2024
Department of Architecture and Civil Engineering
Division of Applied Acoustics
Chalmers University of Technology
SE-412 96 Gothenburg
Telephone +46 31 772 1000

Cover: 3D ray-tracing model of an ice hockey hall constructed in COMSOL Multiphysics®.

Typeset in LaTeX
Gothenburg, Sweden 2024

Influence of temperature gradients on the sound field in ice halls

ALEXANDRA PAPPA
Division of Applied Acoustics
Department of Architecture and Civil Engineering
Chalmers University of Technology

Abstract

This thesis studies the way that temperature gradients affect the sound field in ice hockey halls. This is achieved through reverberation time evaluation. The motivation behind this investigation is found in recent measurements in an ice hall. Substantial differences in reverberation times were observed when the hall was in operation in comparison to the hall without an established ice surface. The differences were mainly located in the low and middle frequency range. The aim of this thesis is to explore and identify the reasons behind this phenomenon. It is assumed to be linked to the temperature gradient, formed due to the presence of ice, that leads to refraction.

To further investigate this hypothesis, new reverberation time measurements are carried out in three ice hockey halls. They are accompanied with air temperature measurements, to enable the temperature gradient estimation. Additionally, COMSOL Multiphysics® is used to simulate one of the halls in order to showcase the effects of refraction and calculate the reverberation time. Finally, measurement and simulation results are compared for the case with and without ice on the ground of the rink. Some conclusions are then drawn regarding the nature of the phenomenon and possible modifications are considered.

Keywords: reverberation time, ice hockey, T_{20}, temperature gradient, room acoustics, geometrical acoustics, ray-tracing, refraction, COMSOL.

Acknowledgements

I would like to thank Brekke & Strand for giving me the opportunity to work on this topic and specifically my supervisor, Jorge Torres for his assistance in the measurements and overall support. I am also deeply grateful to my examiner, professor Wolfgang Kropp for his invaluable guidance and advice. I would also like to express my appreciation to the postgraduate student Leon Müller for his helpful COMSOL Multiphysics® insights.

A big thanks is due to the staff members of the ice halls who were very welcoming and let us use the halls for the measurements amidst their busy schedule. I am also grateful to Jesper Hörnmark for his assistance during the measurements in one of the halls.

Last but not least, I would like to thank the staff at Applied Acoustics and my fellow students for creating such a warm and inspiring atmosphere and making this time such a pleasurable experience.

Alexandra Pappa, Gothenburg, 2024

Contents

List of Figures vi

List of Tables viii

1 Introduction 2

2 Theory 4
2.1 General sound properties . . . 4
2.1.1 Wave equation . . . 4
2.1.2 Speed of sound . . . 5
2.1.3 Sound pressure, intensity and power . . . 5
2.1.4 Air attenuation . . . 5
2.1.5 Refraction . . . 6
2.1.6 Absorption, reflection and scattering . . . 7
2.1.7 Sound signals and impulse response . . . 8
2.2 Room acoustics approaches and reverberation time . . . 8
2.2.1 Wave-based . . . 8
2.2.2 Statistical . . . 9
2.2.3 Geometrical . . . 10
2.3 Reverberation time measurements . . . 11

3 Measurements 13
3.1 Setup and procedure . . . 13
3.1.1 Case study 1 . . . 13
3.1.2 Case study 2 . . . 15
3.1.3 Case study 3 . . . 15
3.2 Results . . . 16
3.2.1 Case study 1 . . . 16
3.2.1.1 Reverberation time . . . 16
3.2.1.2 Temperature . . . 21
3.2.2 Case study 2 . . . 22
3.2.2.1 Reverberation time . . . 22
3.2.2.2 Temperature . . . 23
3.2.3 Case study 3 . . . 24
3.2.3.1 Reverberation time . . . 24
3.2.3.2 Temperature . . . 26
3.2.4 Ice hall comparison . . . 27

4 Simulations **29**
4.1 Preliminary considerations 29
4.2 2D Axisymmetric model 30
4.2.1 Setup 30
4.2.2 Results 31
4.3 3D Models 33
4.3.1 Setup 33
4.3.2 Results 38
4.3.2.1 Constant temperature case 38
4.3.2.2 Graded temperature case 43
4.3.2.3 Graded temperature case without protective glass . . 45

5 Discussion **46**

6 Conclusion **51**

Bibliography **I**

A Appendix **II**

List of Figures

1.1 Reverberation time results from previous measurements 3

2.1 Refraction 6
2.2 Absorption and reflection at wall boundaries 7
2.3 Backward integration decay curve example 12

3.1 Ice hall 1 view and floor plan 14
3.2 Ice hall 1 first measurement setup 14
3.3 Ice hall 2 view and floor plan 15
3.4 Ice hall 3 view and floor plan 16
3.5 Ice hall 1: T_{20} results, all measurements 17
3.6 Ice hall 1: T_{20} and T_{30} results, measurement 1 19
3.7 Ice hall 1: T_{20} and T_{30} results, measurement 3 20
3.8 Ice hall 1: temperature measurement results 21
3.9 Ice hall 2: T_{20} results, all measurements 23
3.10 Ice hall 2: temperature measurement results 24
3.11 Ice hall 3: T_{20} results, all measurements 25
3.12 Ice hall 3: temperature measurement results 26
3.13 Comparative T_{20} results from the first measurement 27

4.1 Calculated sound speed gradient 29
4.2 2D model geometry 30
4.3 2D model mesh 31
4.4 2D model ray trajectories and SPL 32
4.5 3D model geometry 33
4.6 3D model source positions 34
4.7 3D model receiver positions 35
4.8 3D model wall boundaries 36
4.9 3D model mesh, constant temperature case 36
4.10 3D model mesh, graded temperature case 37
4.11 3D model geometry without protective glass 37
4.12 Ray location and SPL from the constant temperature 3D model, with the source at position 1 38
4.13 Ray location and SPL from the constant temperature 3D model, with the source at position 3 38
4.14 Decay curves of the 3D model with constant temperature and parallel rink walls with the source at position 1 39

4.15 Decay curves of the 3D model with constant temperature and parallel rink walls with the source at position 3 40
4.16 T_{20} results from the constant temperature 3D model with parallel rink walls 40
4.17 Schematic representation of the tilted wall configuration 41
4.18 Decay curves of the 3D model with constant temperature and tilted rink walls with the source at position 1 42
4.19 Decay curves of the 3D model with constant temperature and tilted rink walls with the source at position 3 42
4.20 T_{20} results from the constant temperature 3D model with tilted rink walls 43
4.21 Decay curves of the 3D model with graded temperature with the source at position 3 44
4.22 T_{20} results from the graded temperature 3D model 44
4.23 T_{20} results from the graded temperature 3D model without protective glass walls 45

5.1 T_{20} comparison between measurement and simulation - constant temperature case 48
5.2 T_{20} comparison between measurement and simulation - graded temperature case 49
5.3 Comparison between measured T_{20} and simulated T_{20} with parallel rink walls 50

List of Tables

3.1 Ice hall 1: Relative humidity at the five measured heights. 21
3.2 Ice hall 2: Relative humidity at the five measured heights. 24
3.3 Ice hall 3: Relative humidity at the first round of measurements. . . . 26
3.4 Ice hall 3: Relative humidity at the second round of measurements. . 26

4.1 Air absorption coefficient m in m^{-1} for 5 °C and 40% humidity. 30
4.2 3D model source and receiver coordinates. 34

A.1 Frequency-dependent absorption coefficients α of the ice hall materials used in the simulation. II
A.2 Scattering coefficients s of the ice hall materials used in the simulation. II

1
Introduction

Ice hockey halls, like any other type of hall with big volume (concert halls, lecture halls, etc) need special treatment when it comes to sound. That is, among others, in order to ensure that sound is as equally distributed as possible in the room, sound loudness lays between desired levels and the sound signal is clearly audible in all listener positions. Room acoustics is the field of acoustics that studies the sound field in rooms and enhances the listener's experience. One of the most widely used objective metrics to evaluate the sound qualities of a room is its reverberation time (denoted as T, RT or T_{60}). It is defined as the time it takes for the sound to drop to one millionth of its initial value after it is stopped or else for the sound pressure level to drop by 60 dB [1]. Different reverberation times are desired for different types of rooms. For example, the ideal reverberation time of a theatre would be between 0.7 s and 1 s, while in a concert hall it could reach up to 2 s or even more, according to the type of music being performed [1][2]. This thesis tries to investigate the acoustical properties of ice hockey halls through the evaluation of their reverberation time.

Recent measurements in an ice hall (case study 1 for the purpose of this thesis) demonstrated strong differences in reverberation time when the hall was in use in comparison to the hall without an established ice surface. Figure 1.1 presents reverberation time measured at various heights inside the ice rink and also at one position in the audience area. In the left graph, the measurements are performed in the summertime with concrete on the ground of the rink, while in the right one there is an ice surface inside the rink and the measurements are performed during the winter. It can be observed, that in the case of concrete, the results are almost the same regardless of the measurement height. Reverberation time reaches a value of almost 3 s in the low to middle frequency range and drops down to 1 s at 8 kHz. On the contrary, when ice is present, reverberation time is double or even reaching 7 s when measured closer to the ice surface. These higher values are mostly located in the 250 Hz and 500 Hz octave bands. Additionally, there is a clearly visible height dependency in the results. Lower measurement heights seem to yield higher reverberation time values, which decrease substantially at higher measurement points. This long reverberation inside the rink affects the players as it hinders speech intelligibility, making it challenging to understand spoken word during games or practice. Furthermore, it contributes to increased loudness levels, which in the longrun can have a significant impact to the players' hearing.

The following explanation is considered as a working hypothesis. Due to the cold ice surface, the temperature is lower closer to the ground and it increases with height.

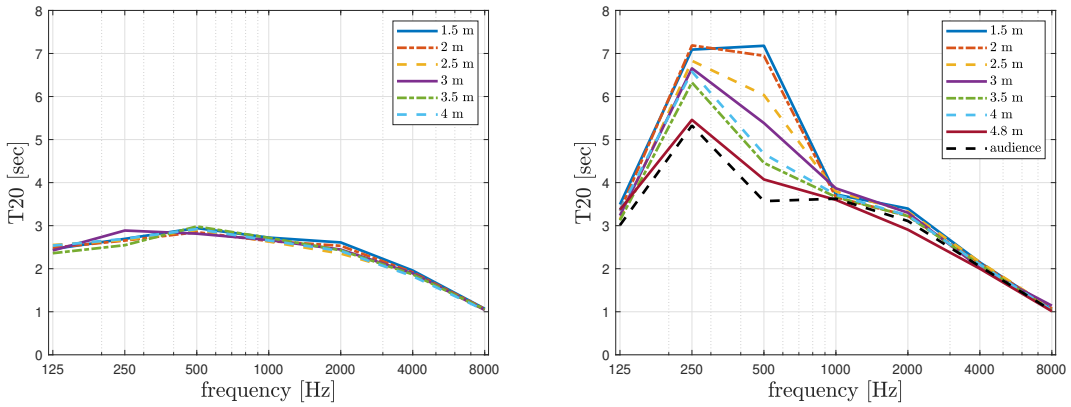

Figure 1.1: Reverberation time (T_{20}) measured at various heights inside the protective glass confined area over concrete (left) and over ice (right)

This temperature gradient leads to refraction of sound. Also, complying with ice hockey regulations, the ice rink is surrounded by protective glass with an average height of about 3 m. Consequently, the energy is unevenly distributed in the hall, as a larger portion of energy is trapped inside the ice rink. Less energy reaches the ceiling and thus the reverberation time is reduced. This is a rather rare case, since typically room acoustics handles rooms with relatively steady temperature values throughout the room volume. As a result, no relevant literature was found.

To further explore this phenomenon, new reverberation time measurements are performed in the aforementioned ice hall and in two more halls to investigate if this is a general occurrence in ice hockey halls. These are accompanied by temperature measurements at various heights to enable the temperature gradient estimation. Additionally, COMSOL Multiphysics® v. 6.1 is used to simulate the first hall and determine whether the phenomenon under consideration can be reproduced through simulation and yield reasonable reverberation time results. COMSOL Multiphysics® is preferred over other room acoustics software, as it is the only one that supports calculations with graded media, translating in graded temperature and speed of sound inside the room.

The Theory chapter of this thesis presents some basic concepts of sound and also explains reverberation time with the help of different room acoustics approaches. Chapter 3 describes the measurement procedure that was followed and presents the reverberation time and temperature results. The models of the simulated hall as well as the simulation results are shown in Chapter 4, while Chapter 5 features an overall discussion of the results. Finally, a conclusion is drawn in Chapter 6.

2
Theory

Since the ice halls under consideration are enclosed spaces, room acoustics methods will be used to study and simulate the sound field. In this chapter, different approaches and room acoustics methods will be presented as well as some relevant sound propagation concepts that provide a better understanding of the discussed topics.

2.1 General sound properties

2.1.1 Wave equation

Sound is propagating in waves through a medium, either fluid or solid [3]. In the context of this thesis this medium is the air. Sound propagation causes a deviation from the static atmospheric pressure, which is called sound pressure. Sound properties in a fluid free of losses can be described by a differential equation called the wave equation [4]. It is comprised by three equations, the equation of motion, the equation of continuity and an equation based on the universal gas law. The resulting wave equation can be written as follows for a plane wave in x direction

$$\frac{\partial^2 p}{\partial x^2} - \frac{1}{c^2}\frac{\partial^2 p}{\partial t^2} = 0 \tag{2.1}$$

p stands for sound pressure, t for time and c is the speed of sound. For a three-dimensional spherical wave, Equation 2.1 will be modified as seen below

$$\nabla^2 p - \frac{1}{c^2}\frac{\partial^2 p}{\partial t^2} = 0 \tag{2.2}$$

where

$$\nabla^2 p = \frac{\partial^2 p}{\partial x^2} + \frac{\partial^2 p}{\partial y^2} + \frac{\partial^2 p}{\partial z^2} \tag{2.3}$$

in Cartesian coordinates. As a solution to the wave equation, sound pressure for a plane harmonic wave can be expressed with Equation 2.4 [3]

$$p(x,t) = \hat{p} \cdot e^{j(\omega t - kx)} \tag{2.4}$$

where $\hat{p}$ is the pressure amplitude, ω the angular frequency and k the wave number.

2.1.2 Speed of sound

The speed of sound depends on the properties of the air. It can be calculated as

$$c = (\gamma RT)^{1/2} \tag{2.5}$$

where γ is the specific heat ratio with the value of 1.4 for air [5]. T represents the temperature in Kelvin. R can be described as follows

$$R = \frac{R_0}{M} \tag{2.6}$$

with R_0 being the universal gas constant with the value of $8314\,\mathrm{J/(Kg \cdot K)}$ and M the average molecular weight. Since dry air consists of 78% Nitrogen, 21% Oxygen and 1% Argon with molecular weight 28, 32 and 40 respectively, M will be 28.96 [5]. Therefore, at 0 °C or 273.15 K, the resulting speed of sound will be $c_0 = 331.37\,\mathrm{m/s}$. Equation 2.7 can be used to calculate the speed of sound in different temperatures [5]. T_C corresponds to temperature in °C.

$$c = c_0 + 0.6T_C \tag{2.7}$$

As a result, for an average temperature of $20°C$ the speed of sound will be $343\,\mathrm{m/s}$, which is the most commonly used value in room acoustics calculations.

2.1.3 Sound pressure, intensity and power

When a source emits sound, its energy is carried by the sound waves. The sound power P or W of the source is defined as the rate of energy transferred per second and is measured in watt (W). The flow of energy is described by the sound intensity I, which is defined as the sound power passing through a specific area perpendicular to the sound wave. [3] Its units are W/m^2 and it can be expressed as

$$\mathbf{I} = p\mathbf{v} \tag{2.8}$$

where $\mathbf{v}$ is the particle velocity. Since $\mathbf{v}$ is a vector, $\mathbf{I}$ is also a vector and it is particularly useful as it shows the direction of energy flow. The relation between power and intensity in a spherical wave can be described as

$$I(r) = \frac{W}{4\pi r^2} \tag{2.9}$$

where r denotes the distance from the source [4]. From the latter equation it can also be observed that intensity is inversely proportional to the square of the distance from the source.

2.1.4 Air attenuation

It has previously been stated that the wave equation describes sound propagation in a lossless medium. However, in reality losses due to air absorption are inevitable not only outdoors, but also inside rooms [6]. As a result, there is an exponential decrease

of the pressure amplitude $\hat{p}$ [3]. For a plane wave propagating in the x-coordinate, this can be described by Equation 2.10

$$p(x) = \hat{p} \cdot e^{-\frac{m}{2}x} \tag{2.10}$$

with m being the attenuation coefficient and x the travelled distance. Consequently, the intensity will be

$$I(x) = I_0 \cdot e^{-mx} \tag{2.11}$$

The air attenuation coefficient is temperature and humidity dependent. It can be found in ISO 9613-1 standard in tabulated form in dB/km for various temperature and humidity combinations and frequencies ranging from 50 Hz to 10 kHz [7].

2.1.5 Refraction

As stated in [4], usually in room acoustics the air is considered as a homogeneous medium and in this case, the sound in high frequencies can be considered to propagate in straight lines as rays, similarly to light. However, sometimes the medium of propagation is inhomogeneous, like the air outdoors or the water. In those cases, differences in temperature and density, amongst others, are observed. As described above, since sound speed depends on temperature, it will be affected by those changes and vary accordingly. Consequently, in cases where the temperature changes with height, thus forming a temperature gradient, there is also a sound speed gradient formed. The change of sound speed leads to curved sound paths, a phenomenon called refraction. Refraction is not common inside rooms, since they tend to have small volumes and their temperature is rather constant. On the contrary, it is quite often observed outdoors, where temperature is prone to changes depending on weather conditions and time of day. The most common case for the temperature outdoors is to decrease with height, leading to a similar decrease of sound speed. As a result the sound rays are curved upwards. The opposite situation takes place when the temperature is low closer to the ground and increases with height (inversion). Therefore, the sound rays bend downwards, as seen in Figure 2.1. The latter is considered to be the case in an ice rink, where there is a positive temperature gradient caused by the cold ice surface.

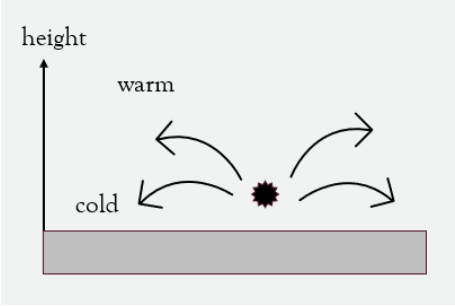

Figure 2.1: Bent sound paths due to temperature inversion

2.1.6 Absorption, reflection and scattering

So far the sound propagation throughout the medium is described. But another important part is the behaviour of the sound when it comes in contact with the boundaries of a room. Walls, furniture or any other obstacles that inhibit sound propagation can be considered as boundaries. Of course, whether or not some object is considered as a boundary depends on the wavelength of the emitted sound wave. Lower frequencies have several meter long wavelengths that can pass through walls, while higher frequencies, with wavelengths of some centimeters or even millimeters, are reflected. As explained in [4], when a sound wave hits a boundary, some of its energy is absorbed and the rest is reflected. Boundary absorption is described by the absorption coefficient α of the material. It is expressed as the ratio of the absorbed energy to the incident energy that reaches the wall.

$$\alpha = \frac{W_{abs}}{W_{inc}} \tag{2.12}$$

α is frequency dependent and can take values between 0 and 1, with 1 indicating total absorption and 0 total reflection. It can either be angle dependent or an average over several angles of incidence [8]. Another absorption parameter used in room acoustics is A, the equivalent absorption area of a room, measured in m^2. All surface areas $S_1, S_2, ...$ and their respective absorption coefficients $\alpha_1, \alpha_2, ...$ are considered in the calculation of A by Equation 2.13 [2].

$$A = \sum Sa = S_1a_1 + S_2a_2 + ... \tag{2.13}$$

The energy that is not absorbed is reflected back to the room. In the case of a completely smooth surface, the energy is reflected specularly. At boundaries with surface irregularities, the energy is reflected diffusely or as a combination of specular and diffuse reflection. In the latter case, the portion of the energy that will be scattered is defined by a scattering coefficient s [8]. Similarly to the absorption coefficient, the scattering coefficient is also frequency dependent and takes values between 0 and 1, with 0 indicating totally specular reflection and 1 totally diffuse reflection.

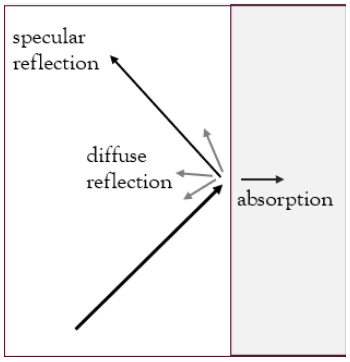

Figure 2.2: Absorption and reflection of the ray's energy after it hits a wall boundary

2.1.7 Sound signals and impulse response

Rooms as well as other acoustical systems like ducts, loudspeakers, etc. are characterized by their impulse response [6]. Each room responds differently to a sound signal depending on several parameters like its specific geometry, boundary conditions, atmospheric conditions, etc. This response can be acquired as an output signal when a room is excited by an impulse signal such as a Dirac pulse. Practically this can be achieved by placing an impulsive source in one position and recording this impulse in another position in the room. Since a room is a linear time-invariant system, an input signal $s(t)$ can be combined with the impulse response $h(t)$ of the room, to obtain the output signal $g(t)$ that would be recorded in the room. This process is called convolution and can be written as

$$g(t) = \int_{-\infty}^{\infty} s(\tau)h(t-\tau)\,d\tau = s(t) * h(t) \tag{2.14}$$

As will later be shown, the impulse response is used to determine the acoustical qualities of a room, such as its reverberation time.

2.2 Room acoustics approaches and reverberation time

Different approaches are used in room acoustics in order to study and explain sound behaviour. This section tries to provide a deeper understanding of reverberation time by viewing it in terms of different room acoustics methods.

2.2.1 Wave-based

One way of studying the sound behaviour in a room is by solving the wave equation for the room's specific boundary conditions [3]. This is a mostly theoretical approach given the complexity of its application in real-case scenarios. However, it is very useful as it allows a realization of the fundamentals of sound behaviour. The wave equation displays non-zero solutions p_q for specific values of the wave number k. For each solution, a certain oscillation pattern representing a standing wave is formed, which is called a room mode. It contains points of zero pressure amplitude and points of maximum pressure amplitude. This built-up of energy leads to resonance at certain frequencies, which are called resonance frequencies. Sound pressure in a rectangular room with no losses can be described as

$$\underline{p}_{q_x q_y q_z} = \hat{p}_{q_x q_y q_z} cos\left(\frac{q_x \pi x}{l_x}\right) + cos\left(\frac{q_y \pi y}{l_y}\right) + cos\left(\frac{q_z \pi z}{l_z}\right) \tag{2.15}$$

q_x, q_y, q_z are natural numbers $0, 1, 2, ...$ and l_x, l_y, l_z represent the dimensions of the room in the x-, y- and z-direction respectively. If a sound wave is propagating in only one direction, meaning that two of the three cosine terms are zero, then this mode is called an axial mode. In the case, where only one cosine term is zero, there is wave propagation in two directions, forming a tangential mode. Three-dimensional propagation is present when none of the terms is zero, leading to an oblique mode.

In cases of losses due to absorption, each mode decays linearly with a damping constant δ. Then, reverberation can be viewed as a superposition of all decaying room modes.

2.2.2 Statistical

Contrary to the wave approach, where the focus is given to the low frequency range, where individual modes can be detected and studied, the statistical approach deals with higher frequencies, where the sound field is more homogeneous due to the contribution of several room modes. This method does not provide an exact description but rather an approximate representation of the sound field [4]. A prerequisite of the statistical method is the presence of a diffuse sound field. This means that the energy has to be evenly distributed across the room. An irregular room shape and a uniform absorption distribution are two factors that contribute to the creation of a diffuse sound field [3]. Since in all real cases there are losses due to absorption, the energy of each mode decays with a decay constant δ according to Equation 2.16 [4].

$$E(t) = E_0 \cdot e^{-2\delta t} \tag{2.16}$$

From the definition of reverberation time, it follows that

$$-60 = 10 \cdot log(e^{-2\langle\delta\rangle}T) \tag{2.17}$$

Hence, reverberation time is

$$T = \frac{3ln10}{\langle\delta\rangle} \tag{2.18}$$

where $\langle\delta\rangle$ denotes the damping constant average [3]. Also according to [4]

$$2\delta = \frac{mc}{2} - \frac{cS}{8V}ln(1-\alpha) \tag{2.19}$$

The first term accounts for atmospheric absorption, while the second corresponds to absorption from the room boundaries. By inserting Equation 2.19 to Equation 2.18, the reverberation time becomes

$$T = \frac{1}{c} \cdot \frac{24Vln10}{4mV - Sln(1-\alpha)} \tag{2.20}$$

This is the famous Eyring equation for calculating the reverberation time of a room. In case of low wall absorption and by omitting atmospheric absorption and inserting $c = 343\,\mathrm{m/s}$, it turns to the commonly used Sabine equation

$$T = 0.161\frac{V}{A} \tag{2.21}$$

where A stands for the equivalent absorption area as defined by Equation 2.13. It has already been stated that for a statistical approach, there needs to be significant overlap of the room modes, such that the sound field is not influenced by individual

mode contributions. According to [3], this happens at a frequency called "Schroeder frequency f_s", which is defined as

$$f_s = 2000\sqrt{\frac{T}{V}} \tag{2.22}$$

For enclosures of large volume this frequency is very low, usually below 50 Hz, permitting smooth acoustics calculations in the frequency range of interest, which starts normally above 125 Hz.

Last but not least, it should be mentioned that in the case where all modes in a room decay with the same damping constant, the decay curve follows a straight line. However, if a group of modes decays with a different damping constant, a decay curve with two or more slopes is created [4]. This happens when two rooms with different reverberation times are coupled together by an opening, as for example in a theatre where the stage and stage house are coupled to the audience area by the proscenium [3]. Coupling can also be observed when the absorption is not distributed uniformly in a room. If there is an area with high absorption and another one with smooth, hard surfaces, the sound field is not diffuse. That means that the energy is unevenly distributed, thus creating two or more sub-spaces with different reverberation times, leading again to double-sloped decay curves [3].

2.2.3 Geometrical

Geometrical acoustics describes sound propagation in similar terms to those used in geometrical optics [4]. Sound waves are depicted as bundles of sound rays with the implementation of the ray tracing and image source methods [3]. This is a high frequency approximation, since the room dimensions need to be large in comparison to the considered wavelengths. It is a simplified approach, as wave phenomena such as diffraction are not taken into consideration. The simulation part of this thesis makes use of the ray tracing method, thus a more detailed description of this method is deemed necessary. As explained in [6] and [3], ray tracing is a stochastic approach contrary to the deterministic image source method. In simulation models using the ray tracing algorithm, an impulse is emitted from the sound source at a certain position in the room, with a predefined sound power and directivity. Rays are simulated as a number of particles moving with the speed of sound. Room boundaries are commonly referred to as "walls". When the rays hit a wall, they are reflected and some of their energy is lost by absorption, according to the respective absorption coefficient of the material. Hence, the energy is decreased by a factor $(1 - \alpha)$. Consequently, the scattered energy is determined by $s(1 - \alpha)$, while the specularly reflected energy is determined by $(1 - s)(1 - \alpha)$. After a particle has hit a wall and is reflected, it continues its travel inside the room. Energy losses can also occur due to air absorption. In that case, the sound pressure decay is defined by Equation 2.10. A particle is traced until a predefined time period has passed or until its power or intensity reaches a specified minimum threshold. Ray tracing has to be performed in all frequency bands within the considered frequency range. Particle energy is detected by a volume detector, typically spherical, which plays

the role of an omnidirectional microphone. It is placed at a certain position inside the room and archives the energy and arrival time of every particle that passes through it. In the end, those stored values are categorized in a histogram also called an "energetic impulse response". It is time-averaged with a common time interval Δt of 1 ms. The obtained impulse response enables the calculation of objective room acoustics metrics such as reverberation time. Crucial for the accuracy of the resulting impulse response is the number of emitted and consequently detected rays. A sufficient number of released rays can be calculated with Equation 2.23 according to [9]. V stands for the enclosure volume and r is the receiver radius, when using a spherical receiver.

$$N_{rays} = 4.34^2 \frac{V}{\pi r^2 c \Delta t} \tag{2.23}$$

The receiver radius and number of rays should be wisely chosen. A small receiver volume could lead to several particles being excluded from the calculation, causing an inaccurate representation of the sound field and misleading results.

2.3 Reverberation time measurements

As explained in [3], reverberation time can be obtained through the impulse response of the room under consideration. This is achieved by recording the sound pressure decay after the room is excited by an impulse signal. Subsequently, the slope of the logarithmic decay curve is used to calculate the reverberation time as seen in Equation 2.24

$$T = 60 \cdot \left| \frac{\Delta t}{\Delta L} \right| \tag{2.24}$$

ΔL stands for the level difference at a specific time interval Δt. There are two methods in use for reverberation time measurements, called interrupted noise method and integrated impulse response method. The first is the most traditional and as described above, is using the recorded decay curve to evaluate the reverberation time. However, due to measurement uncertainty it requires averaging over several measured decay curves. The second method deals with that problem in a more sophisticated way. It was introduced by Manfred Schroeder and employs a backward integration of the squared impulse response defined as

$$bw(t) = \int_t^\infty h^2(t)\, dt \rightarrow bw(n) = \sum_n^{n_{max}} h^2(n) \tag{2.25}$$

with n being the sample number in discrete-time. The measurement procedure is thoroughly explained in ISO 3382-1 [10]. Practically, this method can be implemented by firstly exciting the room with a broadband impulsive signal, e.g. a pistol shot. The decaying sound pressure is then recorded by one or several microphones placed at different positions in the room, yielding the impulse response of the room at each specific position. Then, the reverberation time at each position can be defined by the backward integration method. An octave or third-octave band filter can

be applied to the acquired signal, to enable evaluation at different frequency bands. Afterwards, the impulse response is squared and plotted in a logarithmic scale. An example of such a curve is shown in Figure 2.3.

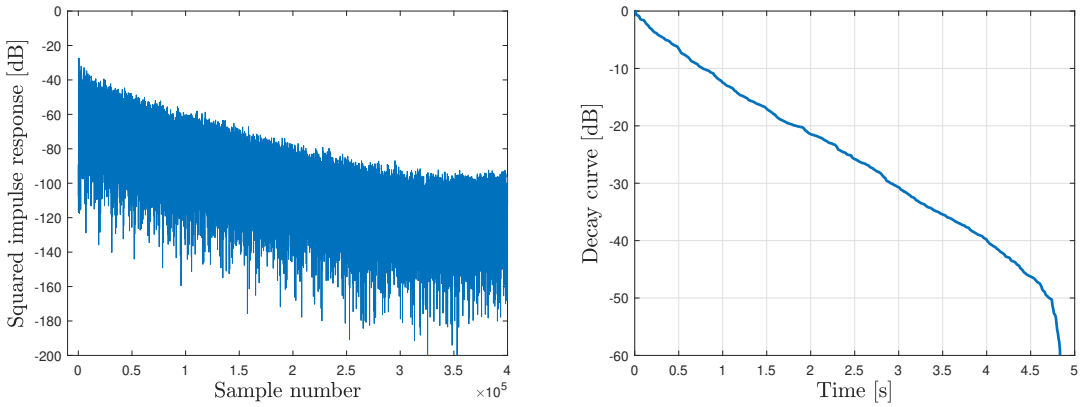

(a) **(b)**

Figure 2.3: Measured impulse response (a) and resulting decay curve using the backward integration method (b).

The part of the curve that falls in the background noise has to be discarded, so that no unnecessary noise affects the accuracy of the calculation. According to the standard, the curve has to be cut at least 10 dB before it reaches the background noise level. As a next step, all values of the curve have to be summed starting from the last until the first. The resulting decay curve, plotted in a logarithmic scale, is also illustrated in Figure 2.3. T_{60} can then be calculated from the slope, using Equation 2.24. A straight line fit may be necessary to reduce random fluctuations. If the dynamic range is not sufficient, as for example in the case shown above, a shorter range can be chosen. Most common is the evaluation of T_{20} or T_{30}, which correspond to a level range of -5 to -25 dB and -5 to -35 dB respectively.

3

Measurements

As mentioned in the Introduction, former measurements in ice hall 1 showed high reverberation times when measured over the ice surface inside the ice rink. It was decided to repeat those measurements together with temperature measurements in order to define the temperature gradient in the hall. The reverberation time measurements were conducted using the integrated impulse response method according to ISO 3382. At the same time, thermometers were used to measure temperature at different heights over the ice surface. This set of measurements was performed in two more ice halls for comparison reasons. This Chapter presents the measurement setup and procedure in each hall as well as the resulting reverberation times and temperatures.

3.1 Setup and procedure

3.1.1 Case study 1

Ice hall 1 is a medium sized hall with a capacity of approximately 3600 seats. A start pistol was used as the sound source for the reverberation time measurements. It was placed in three different positions in the hall, two of which were inside the ice rink and one in the audience area. Six omnidirectional Nor1225 microphones with Nor1209 preamplifiers were used for each source position. Five of the microphones were fixed in different heights inside the ice rink, while the sixth was placed in the seating area. Each microphone was attached to one Nor140 sound level meter. Figure 3.1 presents a view of the ice hall and a plan with the markings of source and receiver positions. Microphones 1-5 were placed above the ice surface at 1.5 m, 2 m, 2.5 m, 3 m and 5 m respectively. Microphone 6 was placed in the audience at a height of 1 m. The reverberation time was firstly measured in all six microphone positions with the source located on the right side of the ice rink, marked as position 1 in Figure 3.1. The setup of this first measurement is displayed in Figure 3.2. The microphones are circled with yellow colour and the source position is marked with red. Each microphone was connected with one Nor140 sound level meter with a built-in reverberation time mode. The integrated impulse response option was selected. This option sets the sound level meter in a waiting mode, until triggered by an impulse sound (e.g. a pistol shot). When triggered, it starts logging and storing the sound pressure level in each frequency band. Once the measurement is finished, it calculates and displays the reverberation time in third octave bands. [11] The recording from each microphone was also saved to be used later for a

manual reverberation time evaluation. Afterwards, the measurement was repeated two more times, with the source moved to position 2, on the left side of the ice rink and position 3 in the audience. A temperature measurement was running in parallel with the reverberation time measurements described above. Five EasyLog USB thermometers were used and mounted on the same bar as the microphones at 0.5 m, 1 m, 1.5 m, 2.5 m and 5 m height. The thermometers were turned on, logging temperature and humidity during the whole time of the measurements.

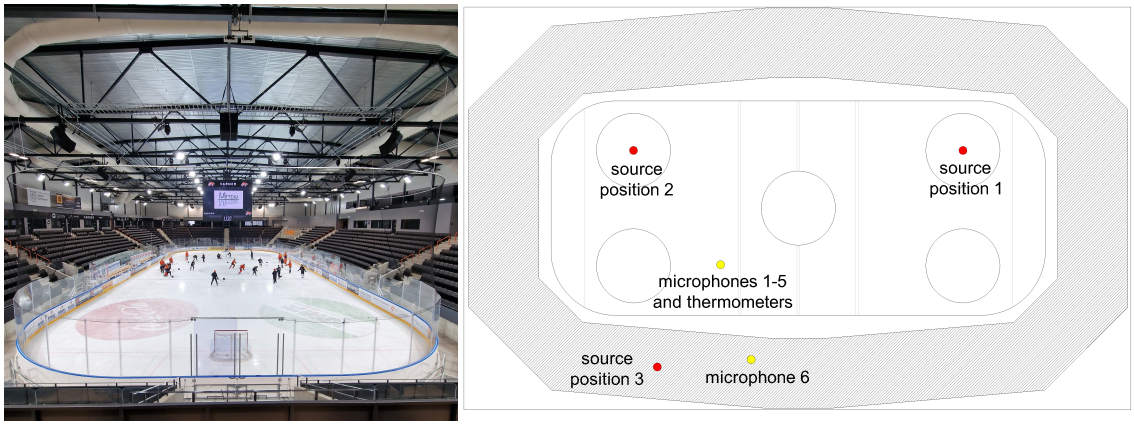

(a) **(b)**

Figure 3.1: Ice hall view (a) and floor plan with marked source, microphone and thermometer positions (b)

Figure 3.2: First reverberation time measurement setup. Receiver positions are marked with yellow and source position is marked with red

3.1.2 Case study 2

Ice hall 2 has a bigger volume that ice hall 1 and it can accommodate 5300 spectators. The reverberation time measurements were performed in a similar way and with the same equipment as in the first hall. Source and receiver positions are marked on the floor plan in Figure 3.3. In this case only five of the microphones were used, all located at the same spot inside the ice rink at the heights of 1.5 m, 2 m, 2.5 m, 3 m and 5 m, each of them being connected to a Nor140 sound level meter. A start pistol was again used as the source signal. The first two measurements were performed with the source located on the right and left side of the ice rink (numbers 1 and 2 in Figure 3.3), while for the third measurement, the source was located in the audience area. The same five EasyLog USB thermometers were used for the temperature measurement, placed at the same spot on the ice as the microphones, at 0.30 m, 0.70 m, 1.25 m, 2.50 m and 5 m. This time, it was decided to measure closer to the ice surface, hence the first three thermometers are placed lower than in case study 1. The thermometers were logging temperature values per minute for the entire duration of the reverberation time measurement, which lasted fifteen minutes approximately.

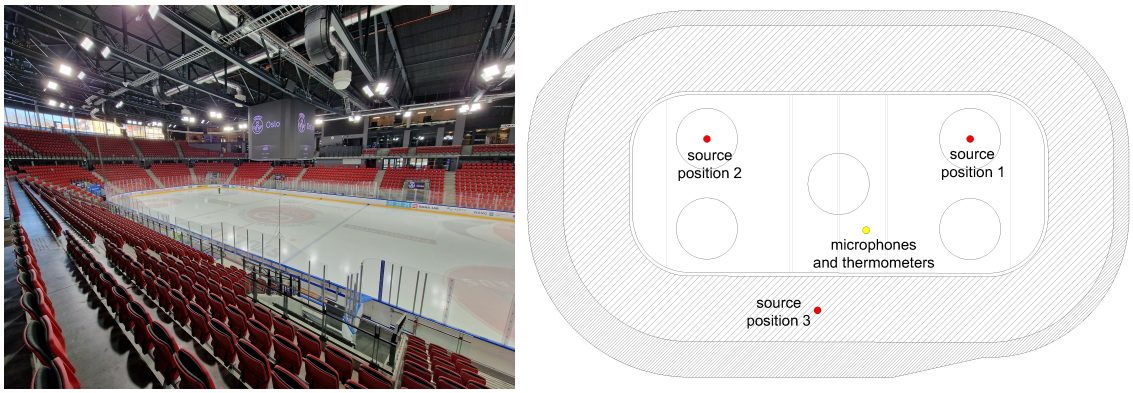

(a) **(b)**

Figure 3.3: Ice hall view (a) and floor plan with marked source, microphone and thermometer positions (b)

3.1.3 Case study 3

Ice hall 3 has a capacity of 6000 seats in the audience area. Some slight modifications were needed this time in the measurement procedure due to equipment availability. Only one Nor140 sound level meter was used, therefore the corresponding microphone had to be moved and placed at the different heights needed. It was decided to measure reverberation time at only three heights instead of five, to reduce microphone position changes. The heights used were 1.5 m, 2.6 m and 5.1 m. Moreover, the source signal was generated by balloons instead of a start pistol. As far as the temperature measurements are concerned, the same five thermometers were used and placed on a long tripod over the ice surface. Microphone, source and

thermometer positions are marked on the floor plan in Figure 3.4.

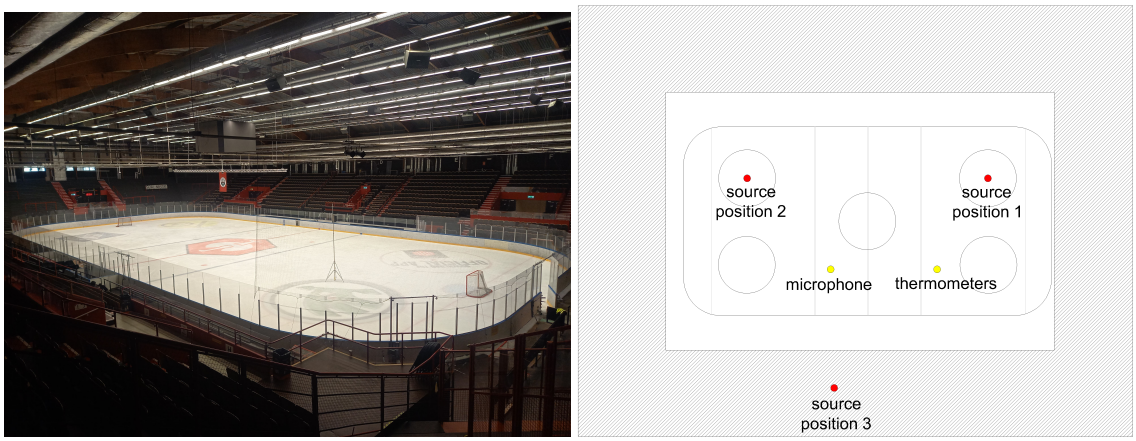

(a) **(b)**

Figure 3.4: Ice hall view (a) and floor plan with marked source, microphone and thermometer positions (b)

Since this ice hall was available for measurements for a much longer period of time than the two previous ones, it was considered wise to leave the thermometers inside the ice rink for an hour to make sure that steady and thus reliable temperature values would be achieved. Afterwards, they were moved to lower positions, in order to obtain results from more points. For the first hour of the measurement, the thermometers were placed at 0.40 m, 0.80 m, 1.35 m, 2.60 m and 5.10 m. For the next half hour, the four lower thermometers were moved to lower heights. The new heights were 0.15 m, 0.30 m, 0.70 m and 1 m.

3.2 Results

3.2.1 Case study 1

3.2.1.1 Reverberation time

The measured reverberation time (T_{20}) as was obtained by the six sound level meters is presented in Figure 3.5. The graph at the top represents the first measurement, where the source was located inside the ice rink, on the right side. Similarly, the middle one shows the results from the second measurement, where the source was located on the left side of the ice rink. For the third measurement, the source was placed in the audience area and the results are displayed in the bottom graph. When looking at T_{20} values from the first two measurements, a similar trend can be noticed in both cases. Starting with a T_{20} value of almost 3 s at low frequencies, there is a significant wide peak around 400 Hz, where T_{20} reaches 7 s at the lowest microphone position (1.5 m). At 1 kHz, T_{20} has fallen back to 3 s, gradually decaying further with rising frequency, ending up to less than a second at 10 kHz.

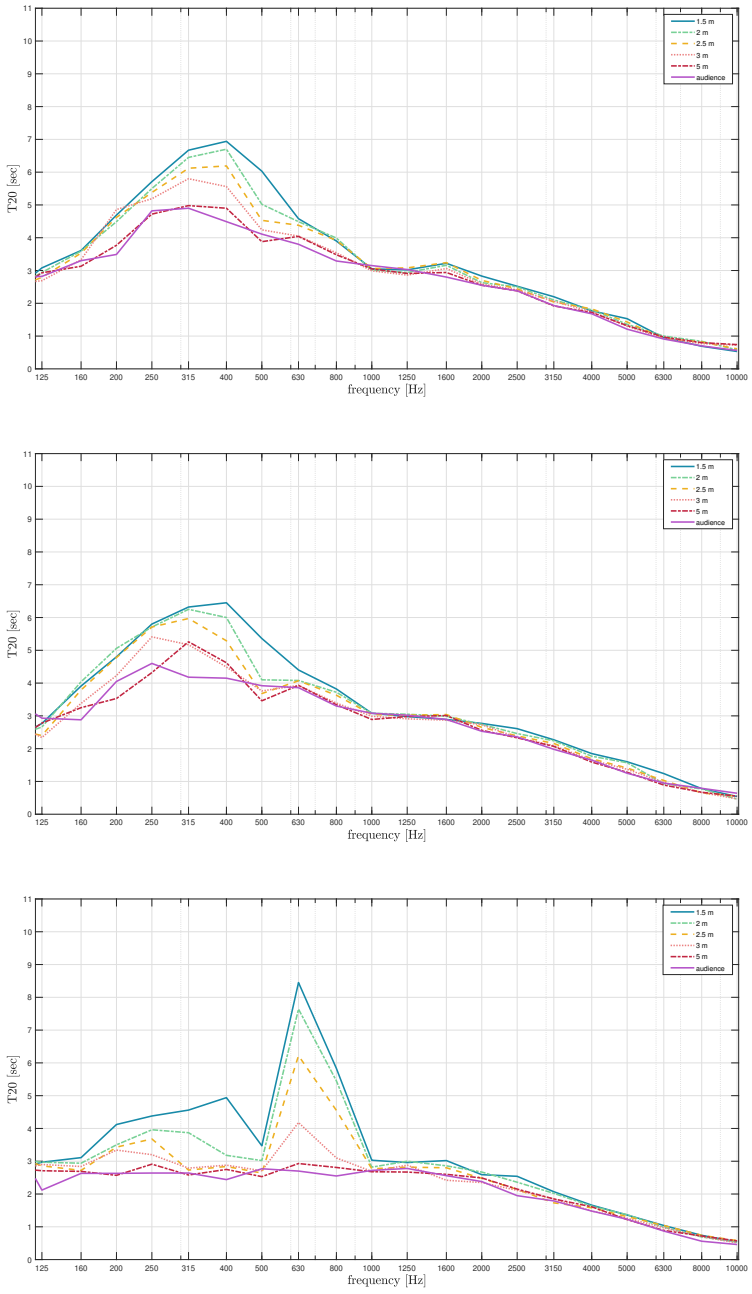

Figure 3.5: T_{20} measured with the sound source in position 1 (top), position 2 (middle) and position 3 (bottom). Each line represents one microphone position. The first five microphones are placed on the ice surface, while the sixth is in the audience area.

This trend is observed over all microphone positions. However, the peak is more prominent when the microphones are placed closer to the ice surface. The highest T_{20} value is measured with the microphone placed at 1.5 m and it decreases inversely with receiver height. At frequencies above 1 kHz, the resulting T_{20} doesn't show any significant dependence on microphone height. By looking at the results of the first two measurements, it is noticeable that they bare a big resemblance to

those of the previous measurements, shown in Figure 1.1. The third measurement shows substantially lower T_{20} values in all receiver positions. The large peak around 630 Hz should not be taken into consideration, as it represents some noise that occurred during the measurement by a double shot of the start pistol. However, this plot is kept and is deemed valuable as it shows the behaviour of the reverberation time when the sound source is located outside the ice rink. The same height dependency is observed as in the two previous cases. However, T_{20} is lower now in all microphone positions. A wide peak between 250 Hz - 400 Hz is more visible in the two lower microphones (1.5 m and 2 m) and less noticeable as the microphone height increases. Another difference from the two previous cases is that T_{20} measured from the 5 m and audience microphones displays no peak but remains rather constant with a value of approximately 3 s over the low and medium frequency range.

T_{30} was also measured and is displayed in Figure 3.6 for the first source position together with T_{20}. The results of each microphone position are presented in separate graphs for easier comprehension. Generally, T_{30} results follow a similar pattern as those of T_{20}. It can be observed that in the results of the lower microphones, shown in Figure 3.6 (a) and (b), T_{20} and T_{30} are almost identical throughout the frequency range. From the 2.5 m microphone onwards ((c) to (f)), T_{30} is higher than T_{20} in the frequency range close to the peak, that is between 200 HZ and 800 HZ. Furthermore, it seems that the difference gets bigger as the microphone height increases. It has previously been stated that T_{20} decreases with height. This tendency is also observed in the T_{30} results, however is can be seen that it decreases with a much slower rate, thus creating the deviation from T_{20} at higher positions, as was previously described. Normally, if the decay curves are straight lines, there shouldn't be any deviation between T_{20} and T_{30}, since they are calculated from the same slope. The fact that T_{30} is higher at some frequencies means that the respective decay curves are double-sloped, thus leading to different results. This kind of curves, seems to be more noticeable in the higher microphones and in the audience.

Figure 3.7 presents T_{30} results from the third measurement, where the source was located in the audience. In this case, the reader should disregard the results between 500 HZ and 1 kHZ, because they are affected by the double shot of the start pistol, as previously explained. In this measurement, where the source was placed in the audience, a different pattern is observed in the T_{30} results. T_{30} is again higher than T_{20} in the frequencies surrounding the peak. However, this difference is more prominent in the lower receivers (Figure 3.7 (a)-(d)). At the 5 m microphone and in the audience, T_{20} and T_{30} seem to be almost identical. It can then be concluded, that with this source placement, double-sloped decay curves are formed mainly in the lower receivers inside the ice rink.

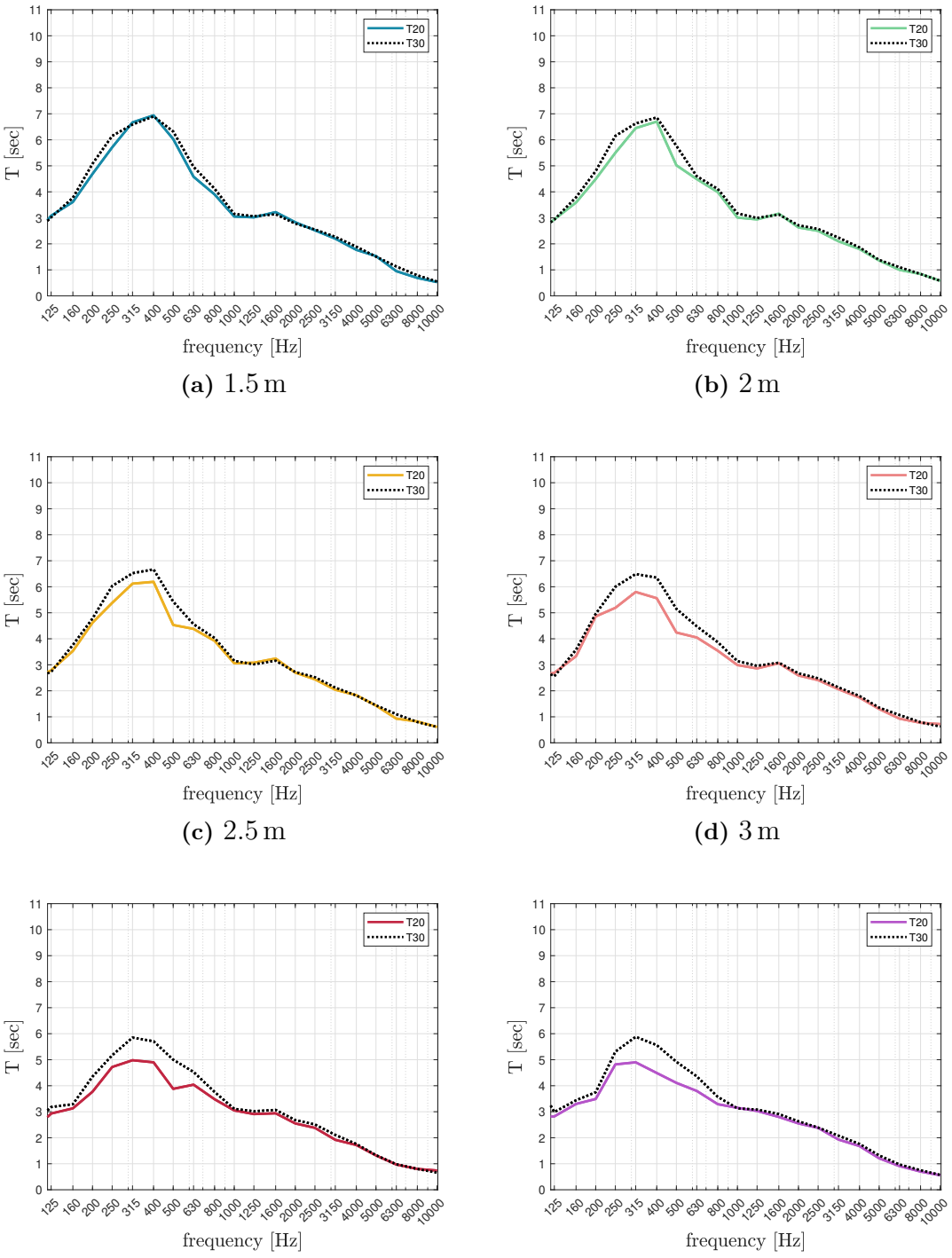

(a) 1.5 m **(b)** 2 m

(c) 2.5 m **(d)** 3 m

(e) 5 m **(f)** audience

Figure 3.6: T_{20} (solid line) and T_{30} (black dotted line) comparison of the results obtained from the first measurement at different receiver placements

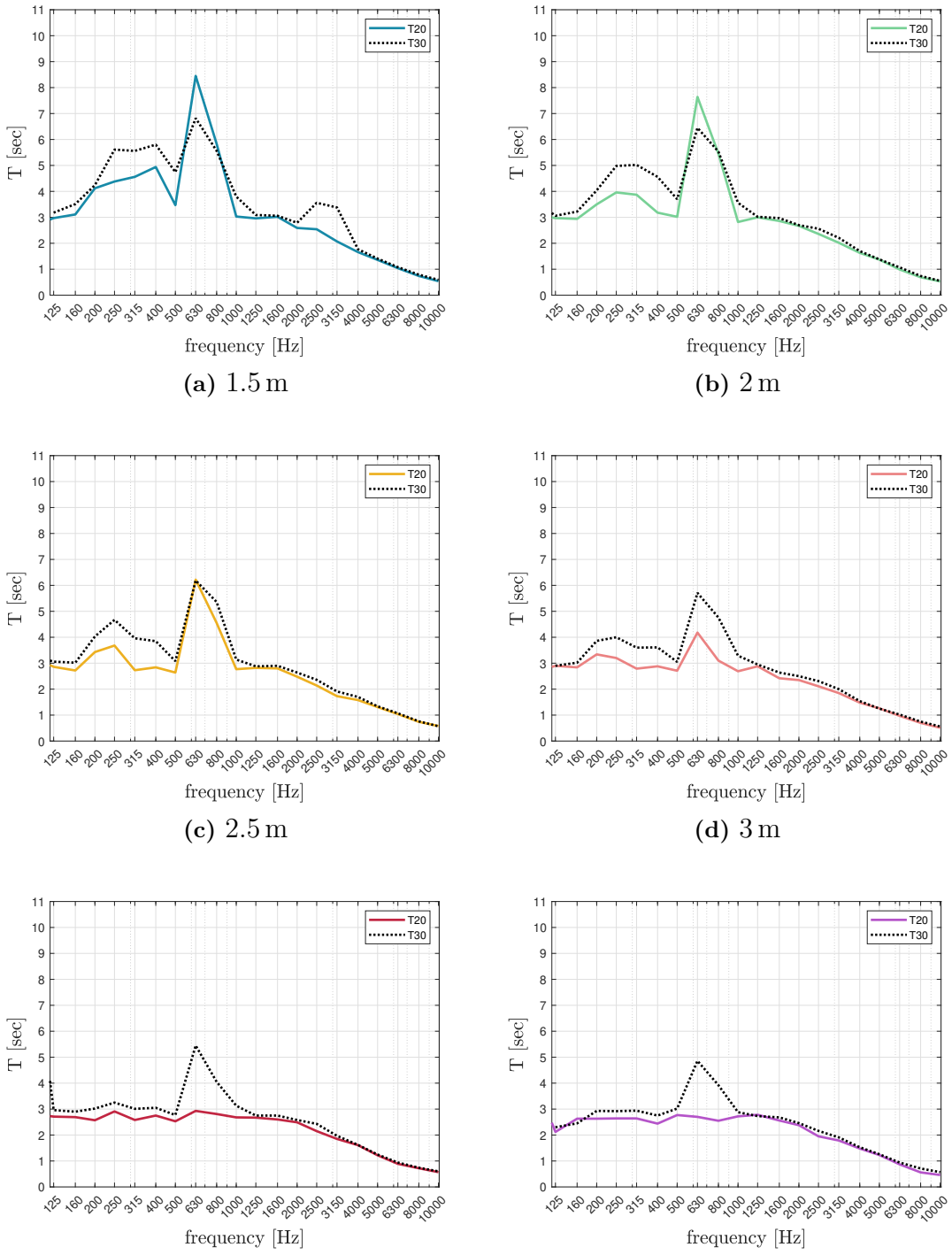

(a) 1.5 m **(b)** 2 m

(c) 2.5 m **(d)** 3 m

(e) 5 m **(f)** audience

Figure 3.7: T_{20} (solid line) and T_{30} (black dotted line) comparison of the results obtained from the third measurement at different receiver placements

3.2.1.2 Temperature

As previously explained, five thermometers were placed at various heights over the ice surface at the same spot as the measuring microphones. They were logging temperature values per minute during the reverberation time measurement. However, the measurement had to be performed within a tight time window, due to various activities that were taking place in the hall. It was observed that by the time the thermometers were removed from the ice rink, the temperature had not yet reached steady values, but seemed that it would continue to drop if the thermometers were left for a longer time in their positions. The final measured temperature values for each thermometer are depicted in Figure 3.8. To estimate the temperature gradient from these points, a least square fit method was used and the resulting curve is also plotted in the same figure.

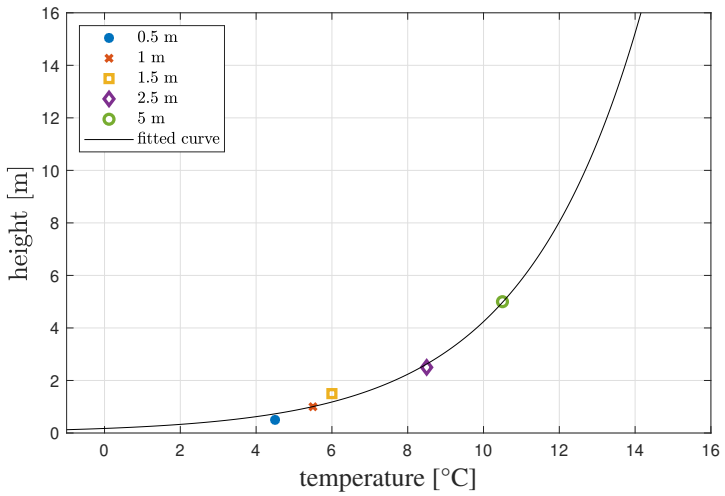

Figure 3.8: Measured temperature at different heights and fitted curve

As expected, the temperature is lower close to the ice surface and increases with height. The temperature gradient follows an exponential growth. However, it should be noted that since the measuring points were located close to the ground, the gradient may deviate a bit at higher points because it is also affected by the outer temperature. As far as humidity is concerned, the three lower thermometers measured values around 51% and some lower values were displayed at higher measurement points. Relative humidity in the five measuring points is shown in Table 3.1.

Table 3.1: Ice hall 1: Relative humidity at the five measured heights.

Height	0.50 m	1.00 m	1.50 m	2.50 m	5.00 m
Humidity	51 %	51 %	51 %	43 %	38 %

3.2.2 Case study 2

3.2.2.1 Reverberation time

Measured T_{20} is illustrated in Figure 3.9 for the three source positions. Similarly to the previous hall, the first measurement with the sound source on the right part of the ice rink is shown in at the top, the second measurement with the source located on the left side of the ice rink is shown in the middle and the third measurement, where the source was placed in the seating area is shown at the bottom plot. For these measurements, all receivers were placed inside the ice rink at the same heights as in ice hall 1 measurements. By looking at all three graphs, it is clearly visible, that T_{20} is height independent from 800 Hz on. At this frequency, it has a value of almost 3 s and gradually decreases as frequencies increase, dropping to 0.6 s at 10 kHz. At frequencies between 200 Hz and 630 Hz there is a big peak in all receiver heights, especially in the first two measurements, where the source was placed inside the ice rink. The peak is more prominent as the receiver height decreases, with T_{20} even reaching the 10 s mark in the second measurement, when measured at 1.5 m above the ice. The location of the peak varies slightly in each microphone, but in general, all microphones have measured high T_{20} values in the aforementioned frequency range. One exception can be found in the third measurement, where T_{20} obtained from the higher microphones, especially the 5 m one, does not display any peak, but stays constant at approximately 2.5 s. The peak effects are also weaker in the rest of the microphones in this measurement and T_{20} is lower overall. Again, the highest value is observed at 1.5 m, but this time it only goes up to 7 s. The rest of the receivers' peak values are below 5 s. The height dependency of T_{20} gets weaker below 250 Hz. Particularly between 125 Hz and 160 Hz there is no noticeable height dependency and T_{20} lies between 2.5 s - 3 s at all measured positions.

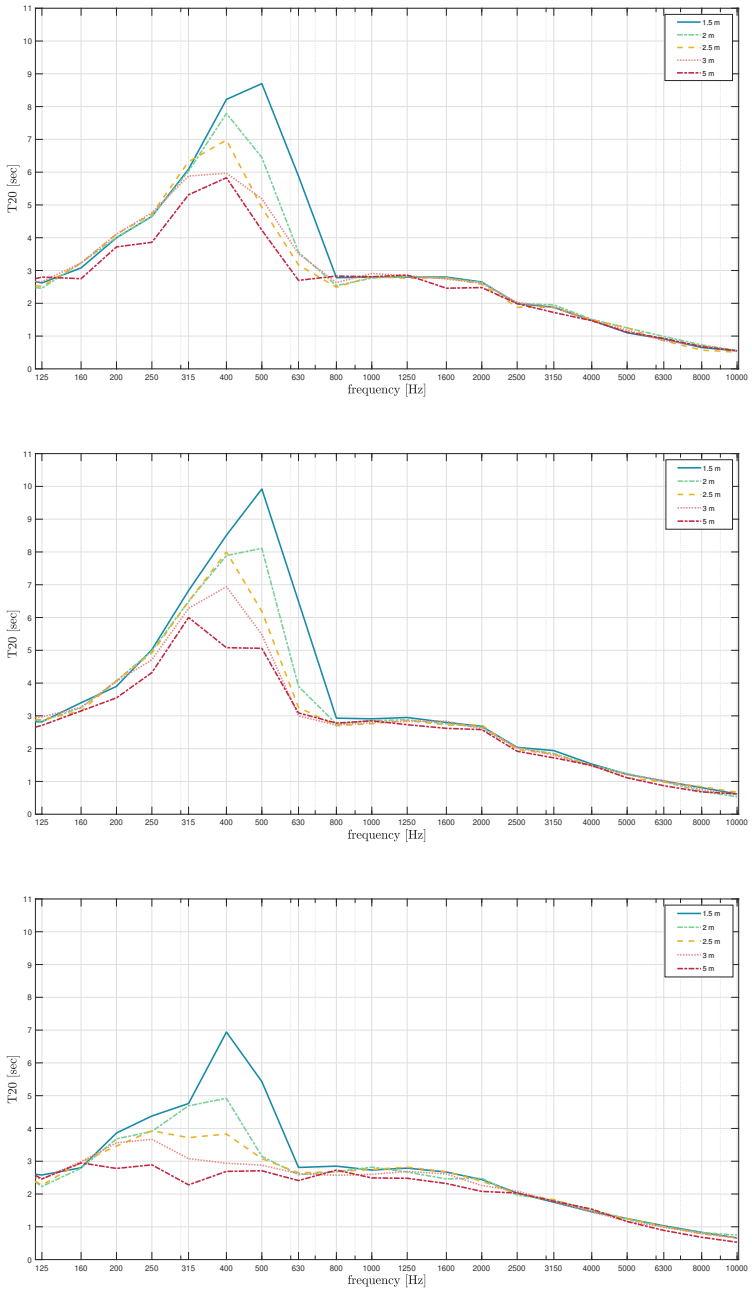

Figure 3.9: T_{20} measured with the sound source in position 1 (top), position 2 (middle) and position 3 (bottom). Each line represents one microphone position. All microphones are placed on the ice.

3.2.2.2 Temperature

Similarly to case 1, it was observed that not all thermometers showed steady temperature values by the time the were removed from their positions. It seemed that especially the lowest ones would measure even lower temperatures if left longer above the ice. Measured temperatures from each thermometer are displayed in Figure 3.10

along with the estimated temperature gradient calculated with the least square fit method. This gradient looks much steeper than the previous one, with the temperature barely reaching 11 °C at 16 m. Relative humidity, measured 15 minutes after the thermometers were placed in their positions above the ice, is shown in Table 3.2. The values lie between 38% and 44%, with the highest humidity found closer to the ice surface.

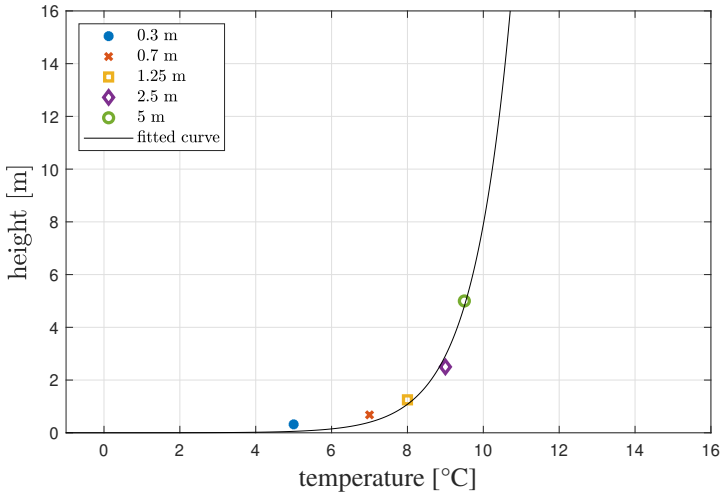

Figure 3.10: Measured temperature at different heights and fitted curve

Table 3.2: Ice hall 2: Relative humidity at the five measured heights.

Height	0.30 m	0.70 m	1.25 m	2.50 m	5.00 m
Humidity	44 %	43 %	41 %	40 %	38 %

3.2.3 Case study 3

3.2.3.1 Reverberation time

As described in the measurement procedure, only three receiver heights were used for reverberation time measurements in this hall, all inside the ice rink. Figure 3.11 shows T_{20} results from the three measurements. Again, as in the previous two halls, the first two graphs represent T_{20} measured with the source on ice, on the right and left side of the rink respectively, while the third graph shows the measurement with the source located in the audience. In the first two measurements, T_{20} falls between 3 s - 4.5 s at frequencies below 200 Hz and above 800 Hz. At higher frequencies, above 1600 Hz, it starts decreasing gradually and finally drops down to 0.6 s at 10 kHz.

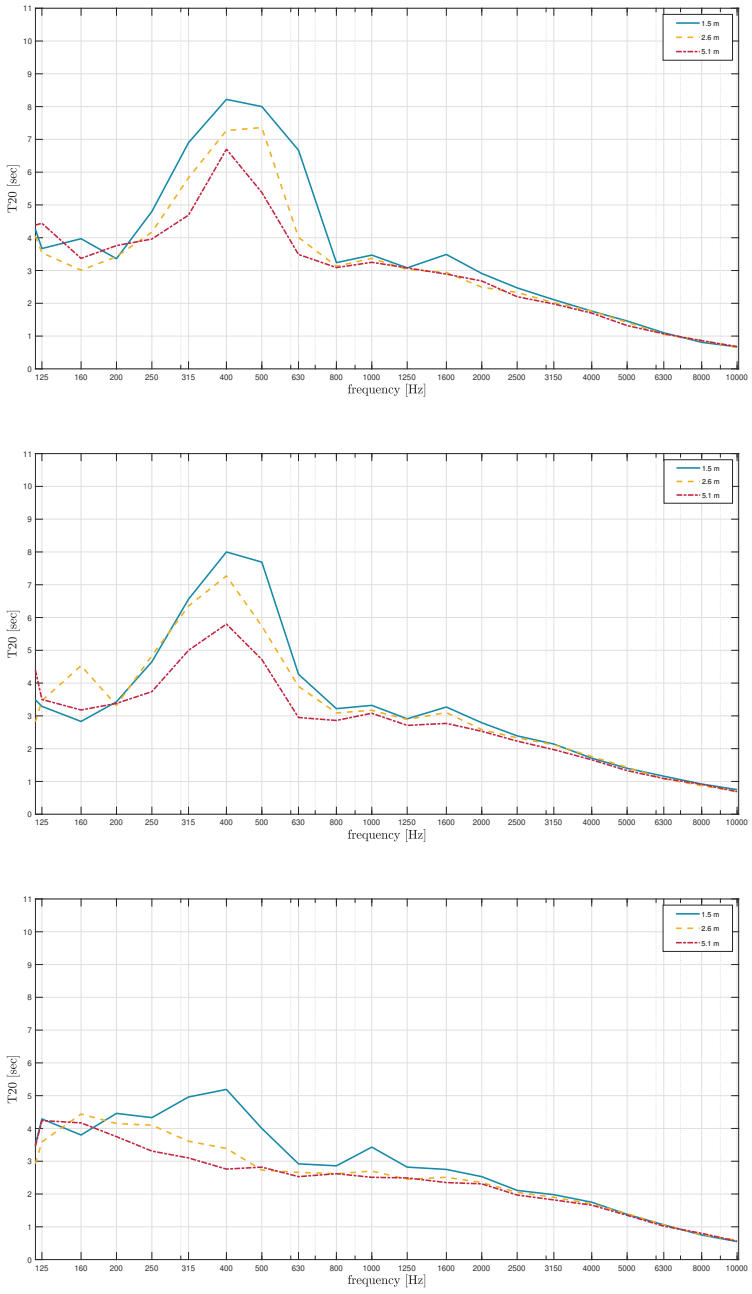

Figure 3.11: T_{20} measured with the sound source in position 1 (top), position 2 (middle) and position 3 (bottom). Each line represents one microphone position. All microphones are placed on the ice.

Between 200 Hz and 800 Hz, there is a significant peak in T_{20} obtained from all three receiver positions, reaching the highest value in the 400 Hz band in the majority of cases. Maximum T_{20} is measured in the lowest microphone position (1.5 m) with a value around 8 s in the first two measurements. Height dependency is again visible, with the results from the middle and highest receiver position (2.6 m and 5.1 m respectively) decreasing by almost 1 s at the peak. As for the third measurement,

T_{20} is much lower mainly in the frequency range where the peak is normally observed (250 Hz - 630 Hz). The peak appears only in the lowest receiver results and reaches 5 s in the 315 Hz and 400 Hz bands. T_{20} curves obtained from the two higher receivers are significantly flatter in this third case. A height dependency is still present, but there is no defined peak.

3.2.3.2 Temperature

As previously explained, more temperature positions were used for the temperature measurements in this hall. Temperature results from all measured points are illustrated in Figure 3.12. The fitted curve is also depicted in the same figure.

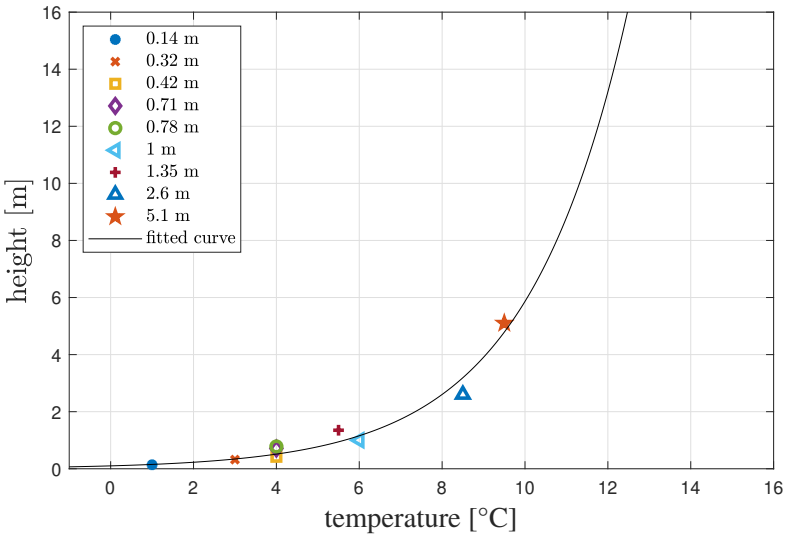

Figure 3.12: Measured temperature at different heights and fitted curve

Tables 3.3 and 3.4 present the relative humidity obtained by the thermometers at the two rounds of measurements. Higher values are primarily observed at lower heights, close to the ice surface.

Table 3.3: Ice hall 3: Relative humidity at the first round of measurements.

Height	0.42 m	0.78 m	1.35 m	2.60 m	5.10 m
Humidity	54 %	56 %	53 %	45 %	42 %

Table 3.4: Ice hall 3: Relative humidity at the second round of measurements.

Height	0.14 m	0.32 m	0.71 m	1.00 m
Humidity	54 %	54 %	56 %	52 %

3.2.4 Ice hall comparison

A direct comparison of the reverberation time of the halls cannot be drawn, since they have very different features (dimensions, geometry, materials) but some general remarks and reflections can be expressed. Figure 3.13 presents T_{20} results from the first measurement in each of the three halls.

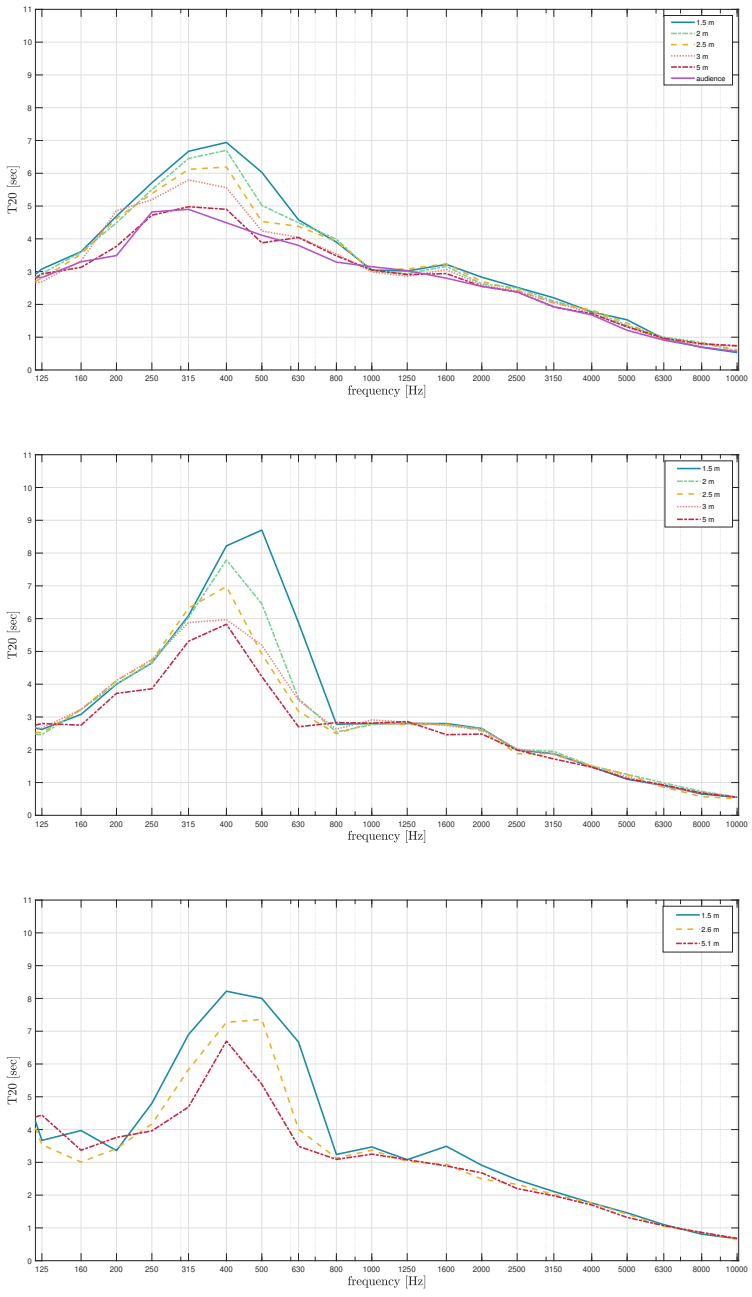

Figure 3.13: T_{20} results from the first measurement setup. Top: ice hall 1, middle: ice hall 2, bottom: ice hall 3

A first observation would be that the reverberation time trend that was observed in

the initial measurements, is not exclusive to ice hall 1 but consistently appears in the rest of the ice hall measurements. It it interesting that the frequency range in which T_{20} is increased is almost identical in all halls spanning from approximately 200 Hz to 800 Hz. The peak is also mostly located in the 400 Hz or 500 Hz third octave band. In addition, it is very clear that T_{20} depends on the height of the receiver and is gradually increasing as the measurement point gets closer to the ice surface. Surely there are some differences in T_{20} values among the halls. In ice hall 2 and 3 T_{20} seems to be around 1 s higher than in ice hall 1 in similar receiver heights. This could be attributed to the bigger volume of those halls, ice rink dimensions, materials and also the sound speed gradient that was affected by the outer temperature at the day of the measurement. Another interesting observation is that in the rest of the frequency range, T_{20} is almost identical in all three halls, with values around 3 s at lower frequencies and above 800 Hz until 2 kHz. After this frequency, T_{20} gradually drops further reaching 0.6 s at 10 kHz as previously described in the measurement results. Additionally, very low or no height dependency is observed at high frequencies.

Regarding the estimated temperature gradients of the three halls, the third one was considered more reasonable, since the thermometers remained above the ice surface long enough to display steady values. Taking into account the fact that ice temperature is almost the same in all halls, this gradient can be considered true for all halls, at least in the immediate vicinity of the ice surface. At higher points, it is also affected by the outside temperature, hence small variations may occur from hall to hall, but also in the same hall when measured at different times of the year. Consequently, the third temperature gradient will be used in the next chapter in the calculation of the speed of sound for the simulations.

4
Simulations

This Chapter presents the models of case study 1 that are created in COMSOL Multiphysics® using the Ray tracing physics interface. Firstly, a 2D Axisymmetric model is created to demonstrate the ray curvature in the graded temperature case and determine whether refraction effects are present in the hall. The ice hall is then simulated in 3D in three different models. The first one shows the case where there is only concrete on the floor of the rink, leading to constant temperature and speed of sound over the hall. The second model represents the case with an ice surface and graded temperature. The third and final model shows a theoretical case where the protective glass walls are removed and the rink area is only defined by the one-meter high wooden board. Firstly the setup of each model is presented, followed by the generated decay curves and resulting reverberation times.

4.1 Preliminary considerations

Some initial parameters had to be calculated based on measurement data before they could be inserted in the models. These include the speed of sound for the graded temperature case and the air attenuation coefficient. Temperature values are necessary to determine the sound speed by Equation 2.7 as presented in the Theory part. As explained in the previous chapter, the estimated temperature gradient from ice hall 3 is employed for the sound speed calculation. The resulting sound speed gradient is depicted in Figure 4.1.

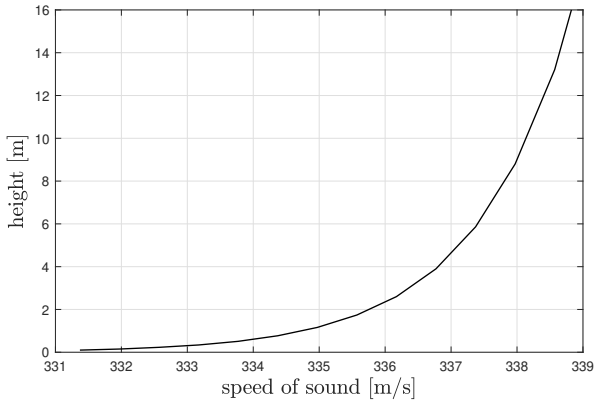

Figure 4.1: Calculated sound speed over height

The air attenuation coefficient m that was used in the models was obtained from ISO 9613-1 standard. It corresponds to 5 °C and 40% humidity. In reality though, temperature and humidity change with height, but these values were chosen for a more accurate representation of the ice rink conditions. Air absorption coefficient in octave bands is shown in the following table in m^{-1}.

Table 4.1: Air absorption coefficient m in m^{-1} for 5 °C and 40% humidity.

125 Hz	250 Hz	500 Hz	1 kHz	2 kHz	4 kHz	8 kHz
$0.51 \cdot 10^{-4}$	$0.1 \cdot 10^{-3}$	$0.2 \cdot 10^{-3}$	$0.7 \cdot 10^{-3}$	$2.6 \cdot 10^{-3}$	$8.3 \cdot 10^{-3}$	$19.5 \cdot 10^{-3}$

4.2 2D Axisymmetric model

The purpose of this model is to examine the ray paths by viewing them in 2D and determine whether the ray trajectories are curved due to refraction effects.

4.2.1 Setup

Only a part of a section of the ice hall is included, since it is considered sufficient for the ray path simulation. The model geometry is shown in Figure 4.2

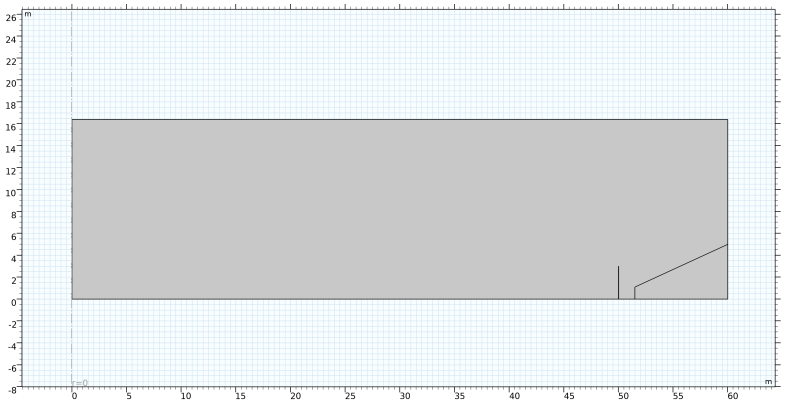

Figure 4.2: 2D model geometry.

The right wall of the geometry represents one of the short walls of the hall. The inclined seating area and the protective glass are also visible on the right side of the geometry. The left wall is the axis of symmetry and it is placed inside the ice rink area. The bottom wall represents the ice/concrete surface. The ceiling is modelled in parallel to the floor, which is not the case in the real hall, but it can be overlooked in this model, as the goal of the computation is the ray curvature at lower heights, inside the ice rink. The Wall Condition is set to Mixed diffuse and specular reflection. The absorption and scattering coefficients of each surface can be found in the Annex. For the axis of symmetry, a Freeze condition is chosen, which means that the rays that hit it are not reflected back. The reason behind this is that this model represents only a part of a section of the hall and the rays that hit the

axis of symmetry would normally continue to travel in the hall, was it modelled in its entirety. The air domain is meshed with a free triangular mesh with a maximum element size of 2.2 m and a minimum element size of 0.1 m. The meshed geometry is illustrated in Figure 4.3.

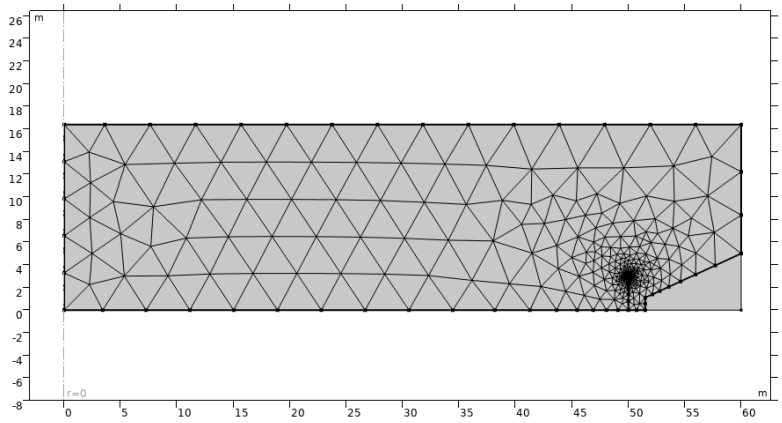

Figure 4.3: 2D model mesh.

The sound source is located on the axis of symmetry at a height of 2 m and has an initial power of 0.03 W. The number of released rays is set to 2000. The computation is performed for the frequency of 500 Hz. The computation time is set to 1 s with a predefined time-step of 0.01 s. For the Fluid model the "User-defined attenuation" option is chosen, where the previously calculated speed of sound and attenuation coefficient are inserted. The default value of 1.2 kg/m^3 is used for the air density parameter.

For comparison purposes, two cases are modelled. The first employs the calculated sound speed gradient with an ice surface inside the rink, while the second uses a constant speed of sound and concrete floor. The constant speed of sound is set to 341 m/s, which corresponds a temperature of 17 °C. For the constant speed of sound, the Intensity computation option is set to "Compute intensity", while for the graded case it is set to "Compute intensity and power in graded media".

4.2.2 Results

Ray paths and SPL for the two modelled cases are shown in Figure 4.4. The two cases are plotted next to each other with the left column representing graded temperature and the right representing constant temperature. Each row corresponds to a different time instant, starting with 0.1 s, then 0.2 s, 0.3 s and finally 1 s. Looking at the first row at 0.1 s, one starts to notice a slight bent of the rays that have been reflected from the ice surface in the first case (left). However, no such bent is visible in the constant temperature case. Here the reflected rays are moving straight upwards. At 0.2 s, the rays on both cases have already reached the protective glass wall and are reflected back in the rink. However, in the graded case they seem to be reflected almost horizontally, while in the constant case they are clearly moving upwards.

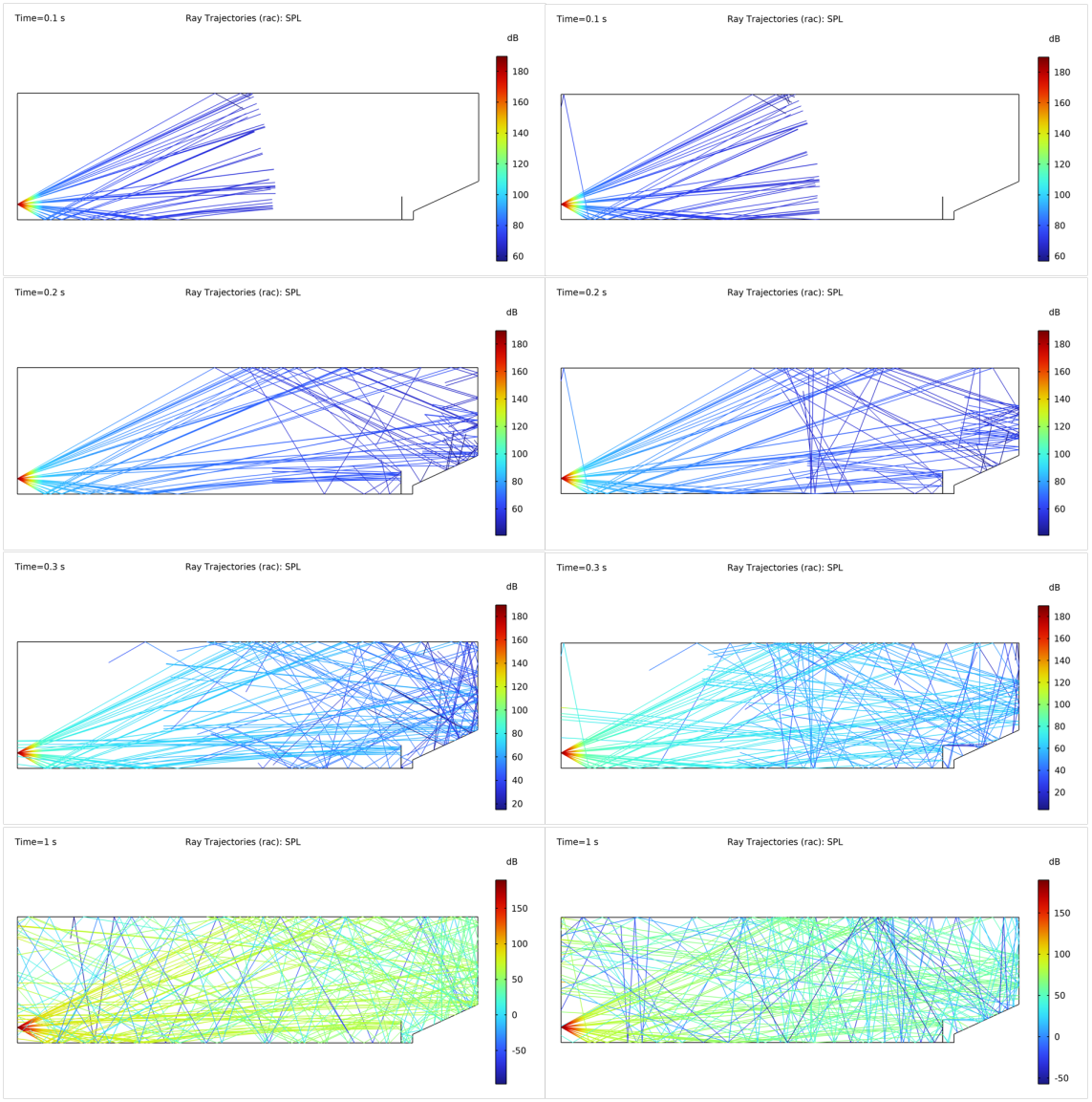

Figure 4.4: Ray location and SPL at 0.1 s (top row), 0.2 s (second row), 0.3 s (third row) and 1 s (bottom row). The left column represents the graded temperature case, while the right column represents a case where the temperature is 17 °C throughout the hall.

Also, in the graded case, the part of the rays that are reflected outside the rink after bouncing back from the ground, seem to land mostly in the seating area and the lower part of the back wall. The situation looks different in the constant case, where the equivalent rays land at the middle part of the back wall, barely reaching the seating area. At 0.3 s, some reflected rays have reached the axis of symmetry on the left side of the geometry. Those rays are positioned much higher in the constant case than in the graded one, where they remain inside the rink. Finally, at 1 s, the total ray distribution in the room can be compared. A noticeably larger amount of rays has remained low, inside the ice rink area in the graded case, while in the constant one they are more evenly distributed throughout the room volume.

4.3 3D Models

The 3D model aims to reconstruct ice hall 1 and use the ray tracing method to calculate the impulse response at different receiver positions. Afterwards, the reverberation time is obtained from the decay curve, as explained in the theory chapter. Three different models are constructed. Firstly, a model to simulate the constant temperature case, where a speed of 341 m/s was used. The second model simulates the graded temperature case, using the previously calculated sound speed gradient. Lastly, the graded temperature case is simulated again, but this time without the protective glass that surrounds the ice rink. This section starts with a general setup, which is common in all cases and proceeds to describe the specific adjustments and results of each case.

4.3.1 Setup

A simplified version of the hall geometry is used. It was initially created in AutoCAD and then imported into COMSOL Multiphysics®. The ice rink is 60 m long and 26 m wide, while the protective glass height is 2.90 m at the long sides and 3.45 m at the short sides. The model geometry is shown in Figure 4.5.

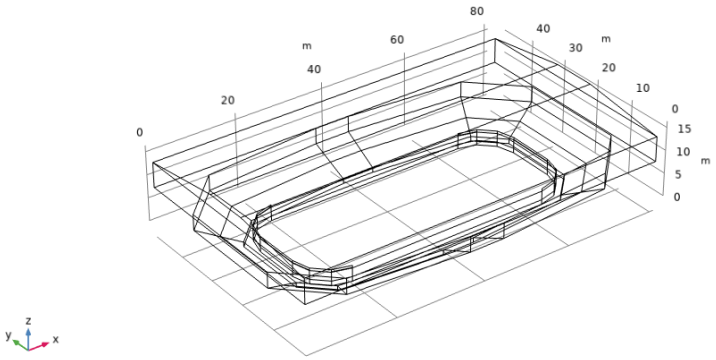

Figure 4.5: 3D model geometry.

The hall volume V is set to 51 600 m^3. The sound source is omnidirectional with an initial power P_0 equal to 0.30 W. Source and receiver positions are chosen to match those used during the measurements. Two source positions are used, one inside the ice rink, similar to position 1 in the measurements and one in the audience, similar to position 3. Three spherical receivers with a 0.6 m radius are used. Two are placed above the ice surface at 1.5 m and 3 m, while the third is located in the audience. All source and receiver coordinates are displayed in Table 4.2. The corresponding positions in the model are illustrated in Figures 4.6 and 4.7.

Table 4.2: 3D model source and receiver coordinates.

Point	x-axis	y-axis	z-axis
Source 1	60 m	32 m	2 m
Source 3	26.5 m	5.5 m	5.5 m
Receiver 1	32.5 m	17.5 m	1.5 m
Receiver 2	32.5 m	17.5 m	3 m
Receiver 3	31.5 m	7 m	4 m

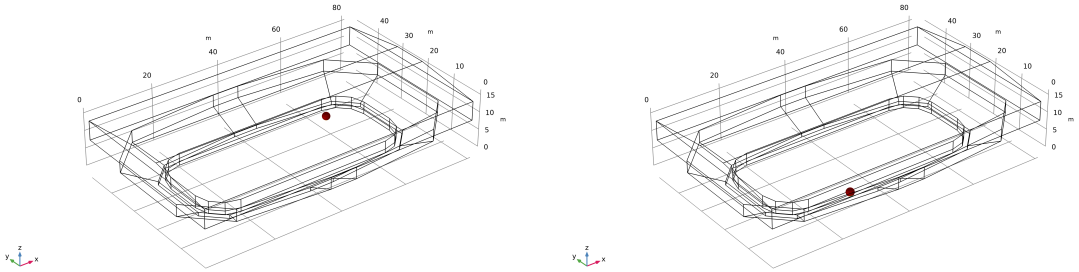

(a) Source 1 **(b)** Source 3

Figure 4.6: 3D model source positions. Position 1 is inside the ice rink and position 3 is in the audience.

The sound speed gradient, air attenuation coefficient, as calculated in Section 4.1, as well as absorption and scattering coefficients of all surfaces are inserted as Interpolation functions under Global Definitions. The Interpolation method is set to Nearest Neighbor. The boundary conditions are defined according to the materials of the different surfaces. Each surface is defined as a Wall boundary in the Ray Acoustics Interface. Mixed diffuse and specular reflection is the selected option under Wall Condition. Consequently, the boundary conditions are defined by the absorption and scattering coefficient of each Wall surface. The surfaces used in the model are ice, wooden board, plexiglass, concrete walls and floor, seating area, plaster walls, Paroc walls, curtain and ceiling. The equivalent area of each material can be viewed in Figure 4.8. The respective absorption and scattering coefficients can be found in the Annex.

There are some structural differences in the models depending on the chosen intensity computation method. When the speed of sound is constant throughout the hall volume, the option "Compute Intensity and Power" is selected. The speed of sound, air density and air attenuation coefficient are inserted in the settings of the Ray Acoustics interface under "Material Properties of Exterior and Unmeshed Domains". This option requires only a surface mesh as the air domain is not taken into consideration. The chosen mesh is free triangular with a maximum element size of 6.48 m and a minimum element size of 0.81 m. A section of the meshed geometry is shown in Figure 4.9, where also the skewness, which represents element quality, is

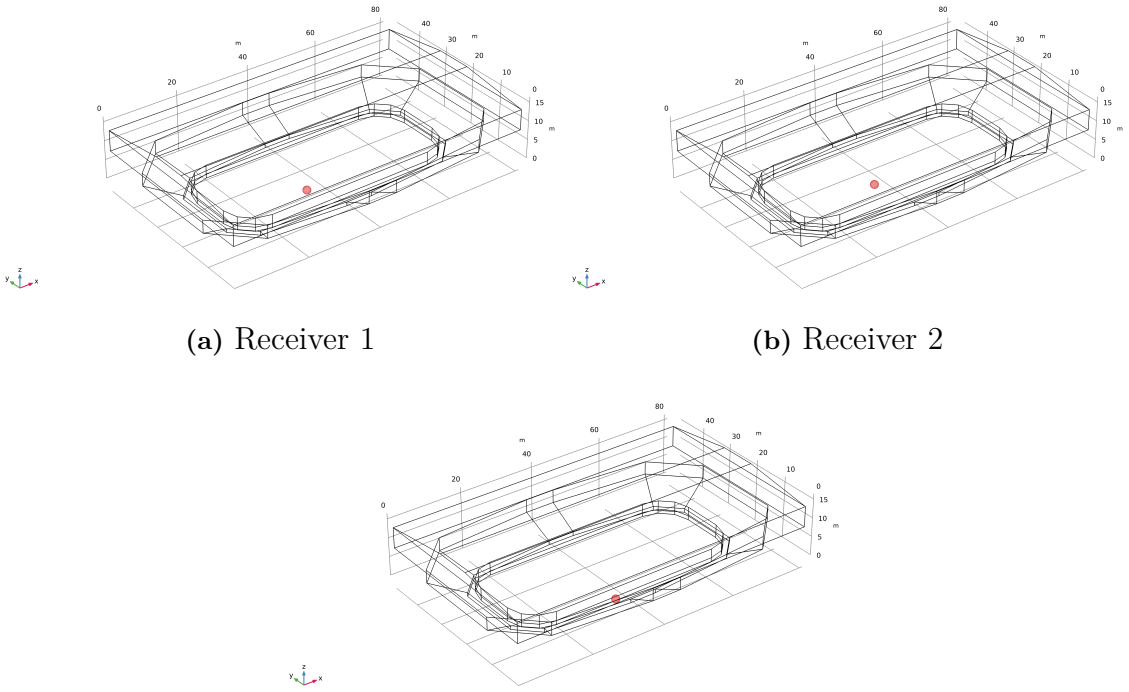

(a) Receiver 1

(b) Receiver 2

(c) Receiver 3

Figure 4.7: 3D model receiver positions. Receiver 1 and 2 are placed above the ice surface at a height of 1.5 m and 3 m respectively. Receiver 3 is in the audience.

depicted. Higher skewness means that the element shapes are regular, contributing to higher mesh quality. It looks like all element shapes of the chosen mesh are sufficiently good for a smooth calculation.

In the case of graded sound speed the intensity computation method "Compute Intensity and Power in graded media" is selected instead. Sound speed as a function of height, air density and air attenuation coefficient are now inserted in the Medium Properties settings, selecting "User-defined attenuation" as the Fluid model. As far as the mesh is concerned, this computation calls for a volumetric instead of a surface mesh, as the air medium has to be taken into account. A free tetrahedral mesh is used with two different sizes. It is finer inside the ice rink with a maximum element size of 1 m and a minimum element size of 0.3 m. The mesh is coarser in the rest of the hall, with a maximum element size of 2.8 m and a minimum element size of 1 m. A section of the meshed geometry and skewness is presented in Figure 4.10.

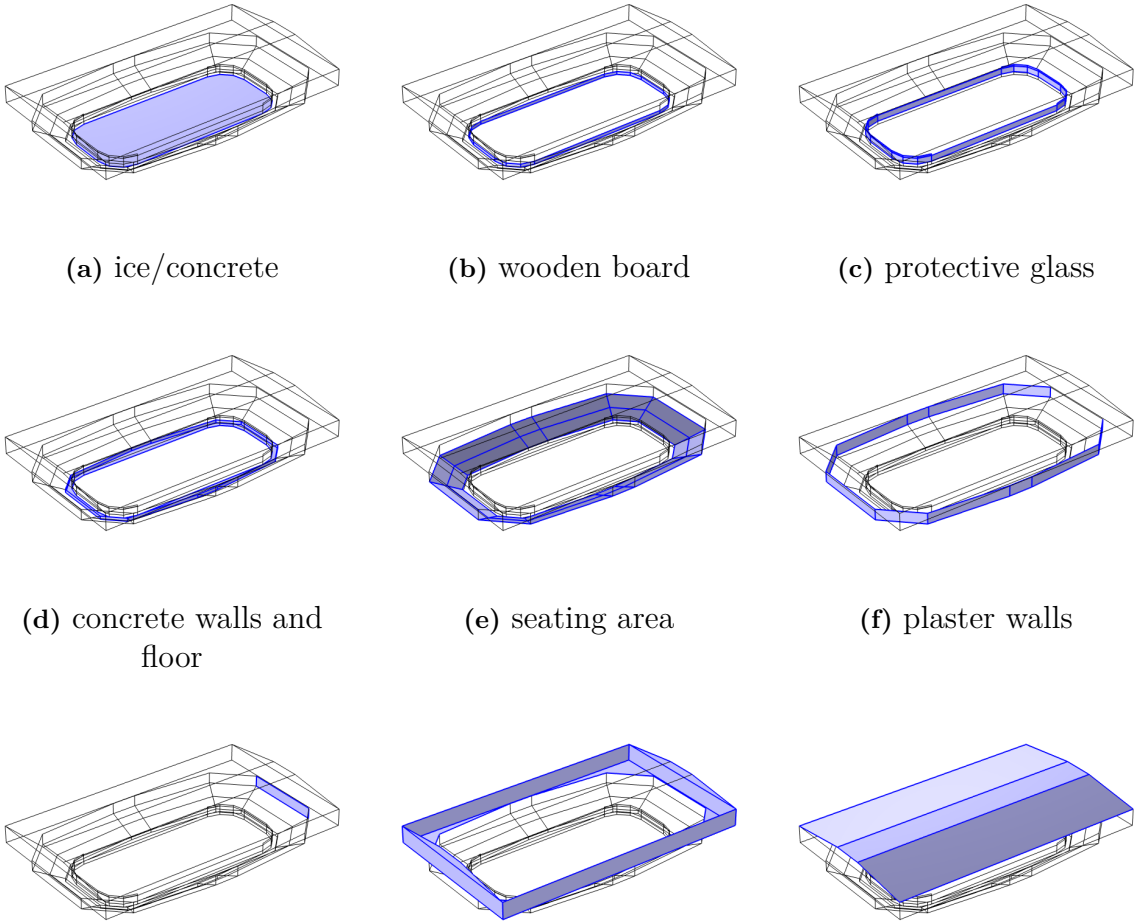

(a) ice/concrete **(b)** wooden board **(c)** protective glass

(d) concrete walls and floor **(e)** seating area **(f)** plaster walls

(g) curtain **(h)** Paroc walls **(i)** ceiling

Figure 4.8: 3D model wall boundaries.

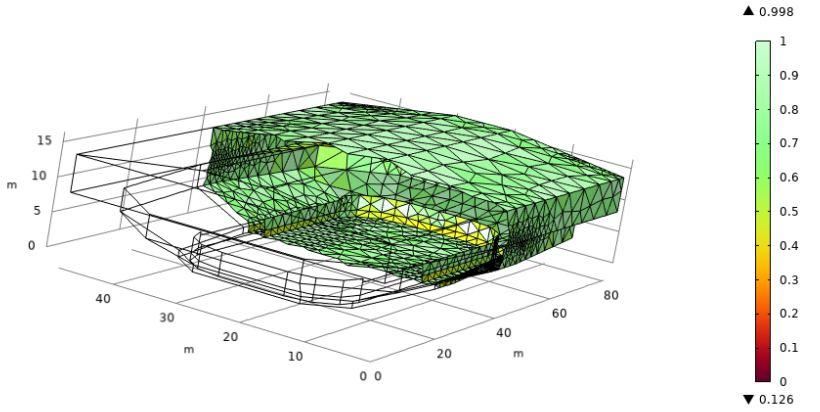

Figure 4.9: Free triangular mesh section and skewness.

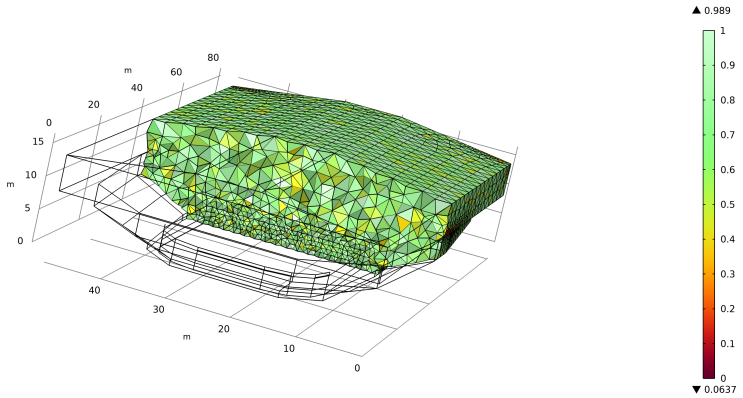

Figure 4.10: Free tetrahedral mesh section and skewness.

The source signal is a parametric sweep in octave bands from 125 Hz to 8 kHz. The computation is terminated when the power of the rays drops to a certain threshold power Q_{th}, which is set to $P_0/N_{rays} \cdot 10^{-9}$ W. The number of emitted rays is determined by Equation 2.23, as explained in the Theory. For $\Delta t = 0.01s$, $c = 331m/s$ and a receiver radius of 0.6 m, N_{rays} equals to 260000. Similarly, in the constant temperature case, where $c = 341m/s$, the number of emitted rays is 253000. As described in the Acoustics module user's guide [9], the Maximum number of secondary rays has to be sufficiently high so as to provide an accurate representation of refraction effects. As a result, a value of 5000 is chosen in the graded case, instead of 500, which was the default option. The end time of the simulation T_{end} is set to 5 s for the constant case and 10 s for the graded case, as longer reverberation times are expected. A time-step of 0.01 s is defined. However, it is expected that the solver will take much smaller time-steps when needed, especially in the beginning of the computation. Furthermore, for the graded temperature case, in the time-dependent solver settings, the Amplification for high frequencies parameter was set at 0.95 instead of the default 0.75 to prevent tolerance-related errors. The modelled case without protective glass has the same setup as the graded case. The difference is that the ice rink area is only defined by the one-meter high wooden board as can be seen in the geometry depicted in Figure 4.11.

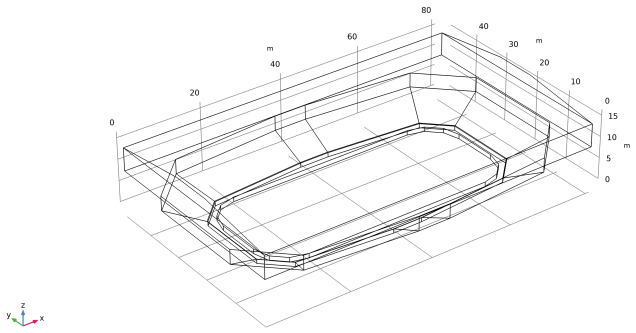

Figure 4.11: 3D model geometry without protective glass.

4.3.2 Results

4.3.2.1 Constant temperature case

Ray trajectories and sound pressure level (SPL) for the 500 Hz band are illustrated in Figures 4.12 and 4.13, computed with the sound source at position 1 and 3 respectively.

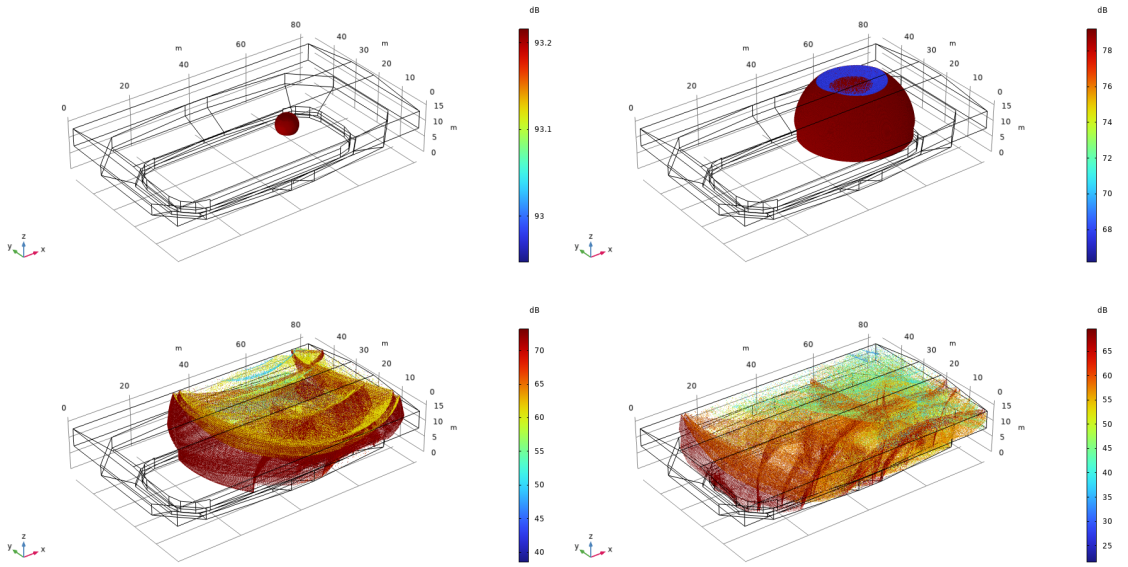

Figure 4.12: Ray location and SPL at 500Hz after 10 ms (top left), 50 ms (top right), 100 ms (bottom left) and 150 ms (bottom right).

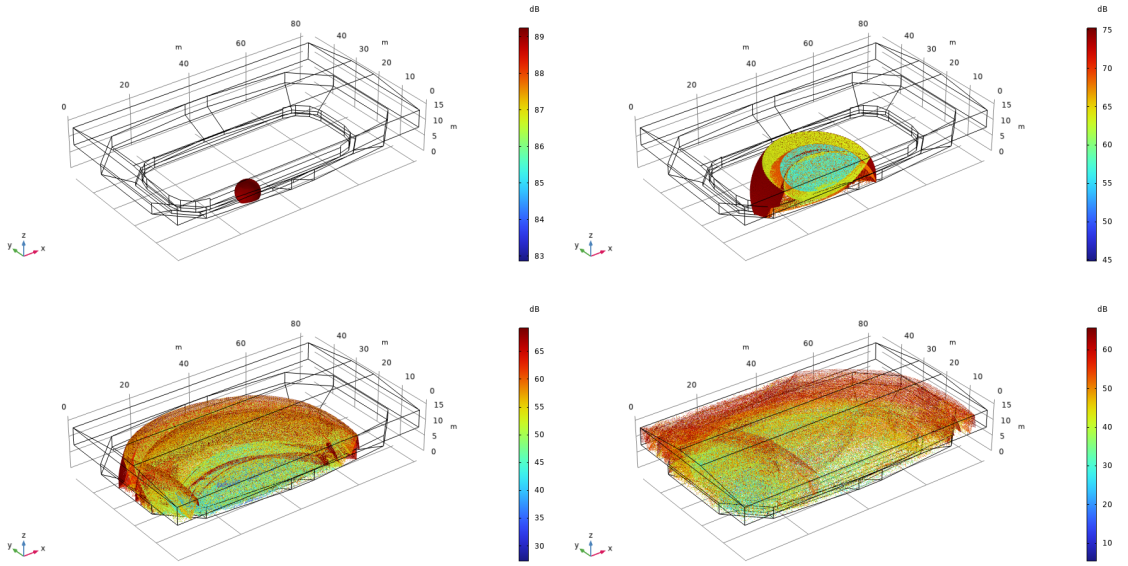

Figure 4.13: Ray location and SPL at 500Hz after 10 ms (top left), 50 ms (top right), 100 ms (bottom left) and 150 ms (bottom right).

Computed decay curves plotted in a logarithmic scale are shown in Figure 4.14 for source position 1 and Figure 4.15 for source position 3. Each plot corresponds to one receiver dataset and includes all seven octave bands used in the calculation. For each set of plots, the two upper ones represent the rink receivers, positioned at 1.5 m (top left) and 3 m (top right). Data from the audience receiver is shown at the bottom plot of each set. The −5 dB and −25 dB points on the y-axis are marked to highlight the T_{20} evaluation range.

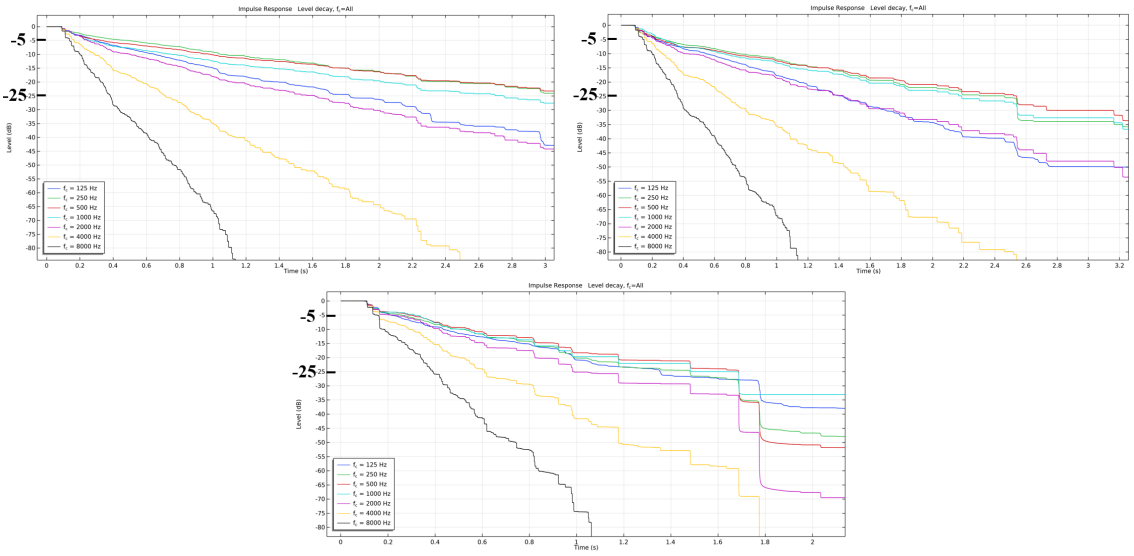

Figure 4.14: Decay curves as computed at receiver 1 (top left), receiver 2 (top right) and receiver 3 (bottom) for the seven octave bands used in the model with the source at position 1.

For source position 1, the decay curves seem to be rather smooth at the level range of interest in all receiver positions, which means that the resolution is satisfactory for the T_{20} evaluation. The curves of higher frequencies tend to be steeper, which indicates lower reverberation time. Although the lines are not completely straight, they can be perceived as single slopes. On the contrary, when the source is positioned in the audience, the resulting decay curves seem to consist of two different slopes, with the steeper one located at the beginning of each curve. This can be observed over all receivers and all frequency bands. Double-sloped curves are more prominent in the audience receiver. The first slope in this case extends over a wider level range with the bent located at approximately −17 dB. This could raise questions as to the accuracy of T_{20} results, as it is evaluated in the range of −5 dB to −25 dB, so the second slope will be mostly disregarded. Another observation could be that the difference between the two slopes is bigger at lower frequencies and less obvious at higher ones.

The resulting T_{20} as obtained by the three receivers with the sound source at positions 1 and 3 is illustrated in Figure 4.16. Looking at the left graph, which represents source position 1, it can be noticed that T_{20} is very high inside the rink. There is a large peak at the 500 Hz band, where T_{20} reaches a value of 7.5 s at 1.5 m, followed by 6.5 s at 3 m. After 1 kHz it falls fast, only to end up less than 1 s at the 8 kHz octave

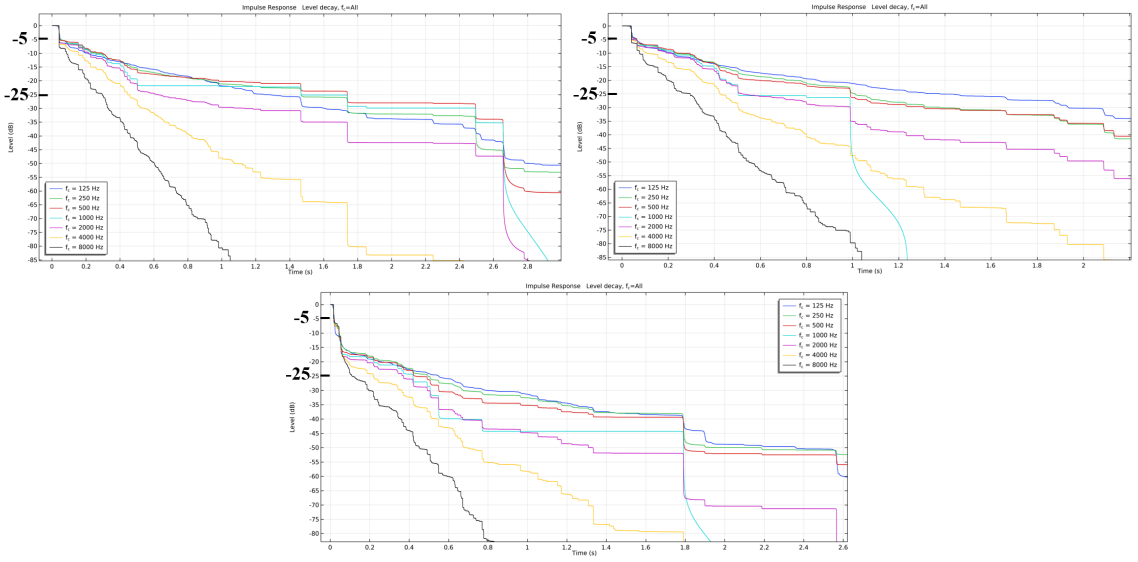

Figure 4.15: Decay curves as computed at receiver 1 (top left), receiver 2 (top right) and receiver 3 (bottom) for the seven octave bands used in the model with the source at position 3.

band. On the other hand, the audience receiver displays constant values in the low to middle frequency range that approximate 3.5 s and falls further at higher frequencies to meet the other two receiver results. Overall lower T_{20} is produced when the source is outside the rink. A height dependency is still observed, with higher values obtained by the lowest receiver position. Here, the peak at 500 Hz reaches up to 5 s and then T_{20} falls down to less than 2 s at 2 kHz. The 3 m receiver shows decaying reverberation time values, starting from 4 s at 125 Hz and falling down to 1.4 s at 1 kHz. The third receiver produces more steady reverberation time around 1.5 s at low and middle frequencies that drops a bit further at higher frequencies.

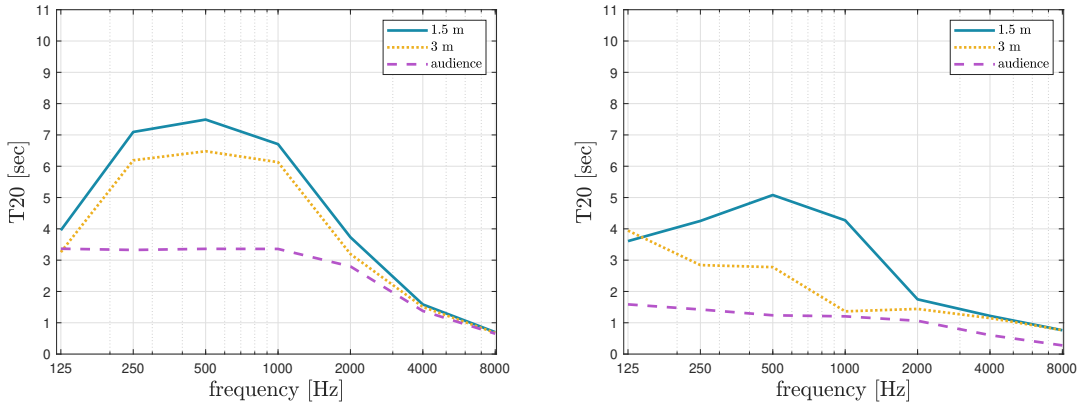

Figure 4.16: Simulated T_{20} with the sound source placed inside the rink (left) and in the audience area (right). Each line represents one receiver. Receivers 1 and 2 are located inside the rink at 1.5 m and 3 m (solid and dotted line respectively), while receiver 3 is in the audience (dashed line).

These results are not at all expected. According to the respective measurements, T_{20} should fall in the range of 2 s to 3 s and be relatively constant. The reason could be that the opposite walls of the protective glass are completely parallel to each other. This probably does not correspond to reality, where such perfectly parallel walls are difficult to achieve. To confirm this assumption, the rink walls were slightly tilted in different directions and angles, to make sure that the sound rays are more evenly distributed. This was achieved by displacing some points at the upper edge of the wall by a few centimeters, as illustrated in Figure 4.17. The arrows point to the direction of the displacement. The black solid lines represent the bottom edge of the wall with the original parallel configuration and the blue dotted lines represent the resulting upper edge of the wall after the displacement. The displacement is very small in reality, but it's exaggerated in the picture for easier comprehension.

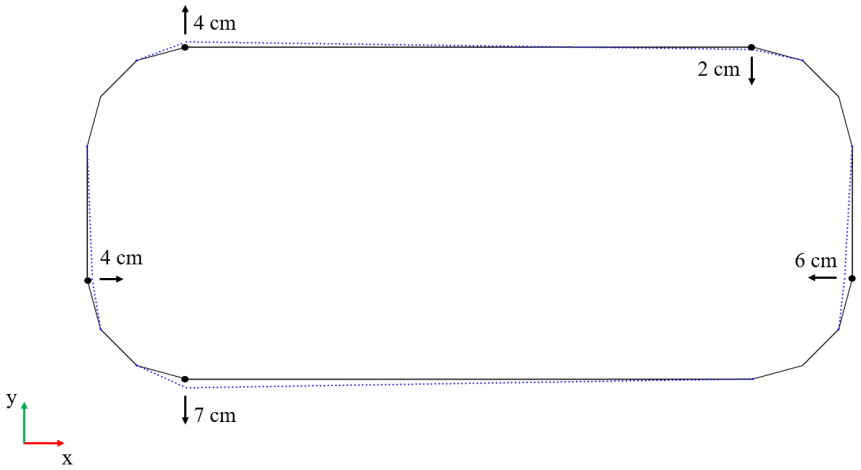

Figure 4.17: Schematic representation of the tilted wall configuration.

The new decay curves for each octave band are shown in Figure 4.18 for the three receiver positions and source position 1 and in 4.19 for source position 3. It seems that with the tilted-wall configuration, the decay curves tend to be single-sloped for both source positions used. Two slopes can only be observed in the decay curves of receiver 1 when the source is located in the audience. The resulting reverberation time is shown in Figure 4.20. T_{20} is significantly lower in both cases. For the first case, where the source is located inside the rink, there is almost no noticeable peak in reverberation time and it spans between 2.8 s and 3.5 s up to 1 kHz at all three receivers. At higher frequencies it falls further, as expected. Similar results are produced when the source is in the audience. T_{20} ranges between 3 s and 4 s at low and middle frequencies, with the audience receiver producing slightly higher values than the previous case. These results resemble more closely the real measurements as shown in Figure 1.1, so this new tilted wall structure is maintained in the following models.

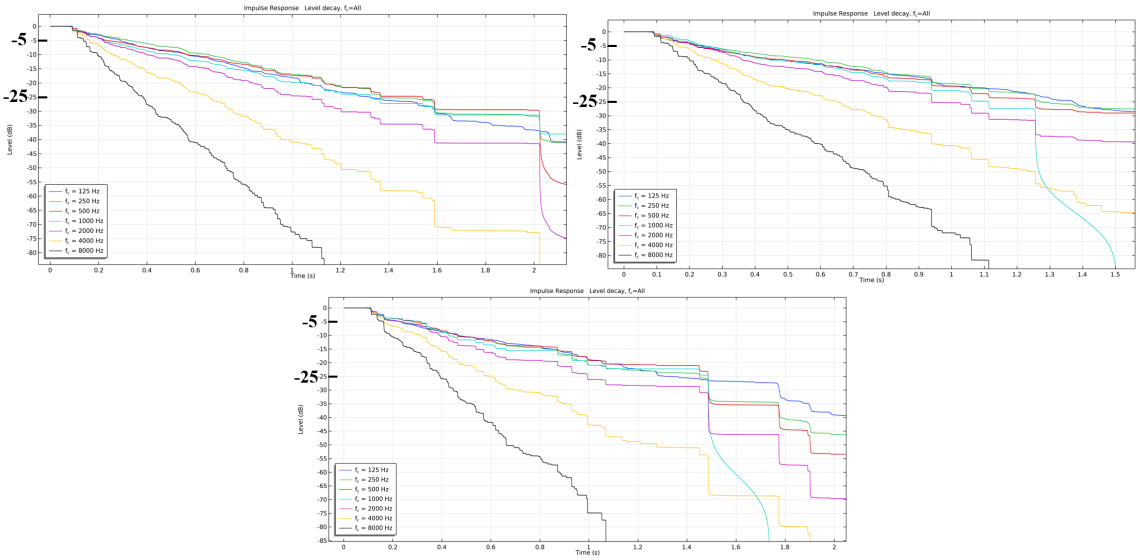

Figure 4.18: Decay curves as computed at receiver 1 (top left), receiver 2 (top right) and receiver 3 (bottom) for the seven octave bands used in the model with the source at position 1 and the tilted ice rink wall configuration.

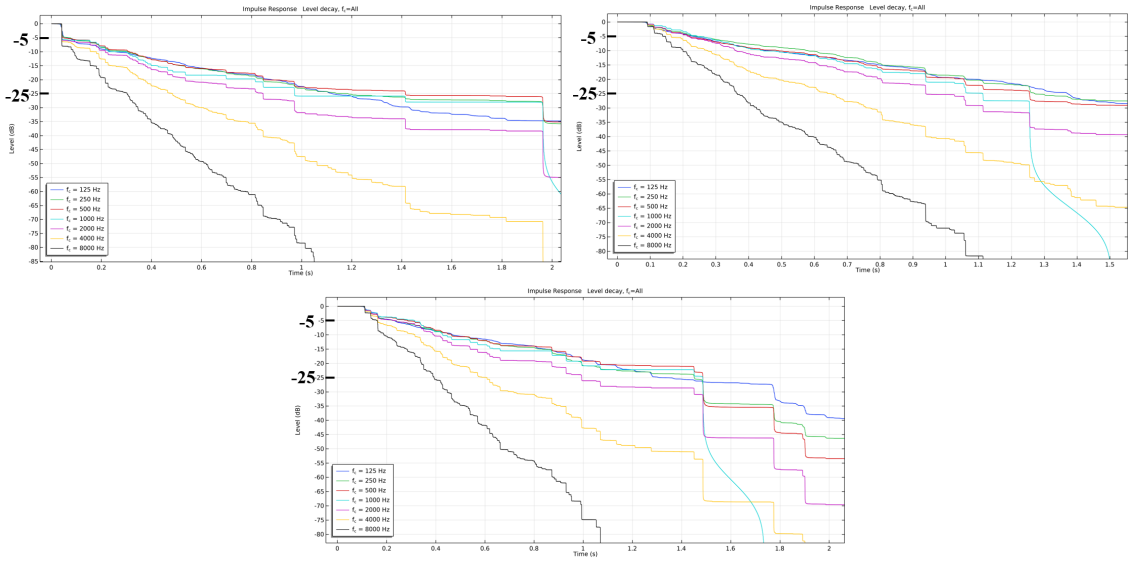

Figure 4.19: Decay curves as computed at receiver 1 (top left), receiver 2 (top right) and receiver 3 (bottom) for the seven octave bands used in the model with the source at position 3 and the tilted ice rink wall configuration.

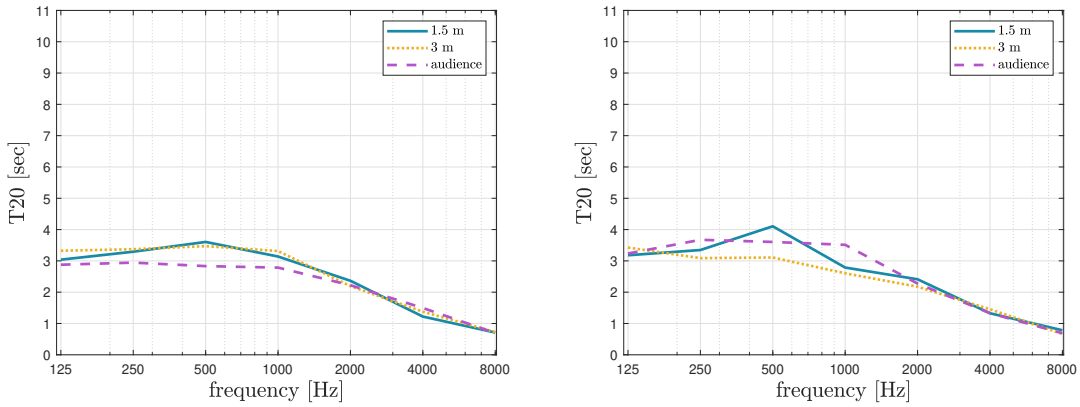

Figure 4.20: Simulated T_{20} with the sound source placed inside the rink (left) and in the audience area (right). Each line represents one receiver. Receivers 1 and 2 are located inside the rink at 1.5 m and 3 m (solid and dotted line respectively), while receiver 3 is in the audience (dashed line).

4.3.2.2 Graded temperature case

Source position 1

Unfortunately, the model configuration with this source placement was very computationally demanding and could not yield results. The solver needed to take very fine time-steps especially in the beginning of the computation and in combination with the high amount of emitted rays, the model file was too large. The RAM memory required to process the impulse responses and render the decay curves exceeded 120 GB, which was more that the computer capabilities.

Source position 3

Since in this case the source is located outside the ice rink, it becomes less computationally demanding for the graded media algorithm as the number of reflections is reduced. Thus, the impulse responses could be computed and reverberation time results could be obtained. However, it was still a cumbersome computation that lasted approximately 60 hours. Resulting decay curves for the three receiver positions and all frequency bands are shown in Figure 4.21. A higher amount of irregularities is observed compared with the constant case. That could have some effect on the accuracy of the resulting T_{20}. Ideally, a higher resolution with a higher amount of rays would be needed for smoother curves. As far as the slope is concerned, is seems that all curves from all receiver positions and all frequency bands exhibit double-slope characteristics. The effect is more pronounced in the decay curves produced by receiver 3. Here, the first slope extends over a wider level range than in the cases where the receivers are located inside the ice rink.

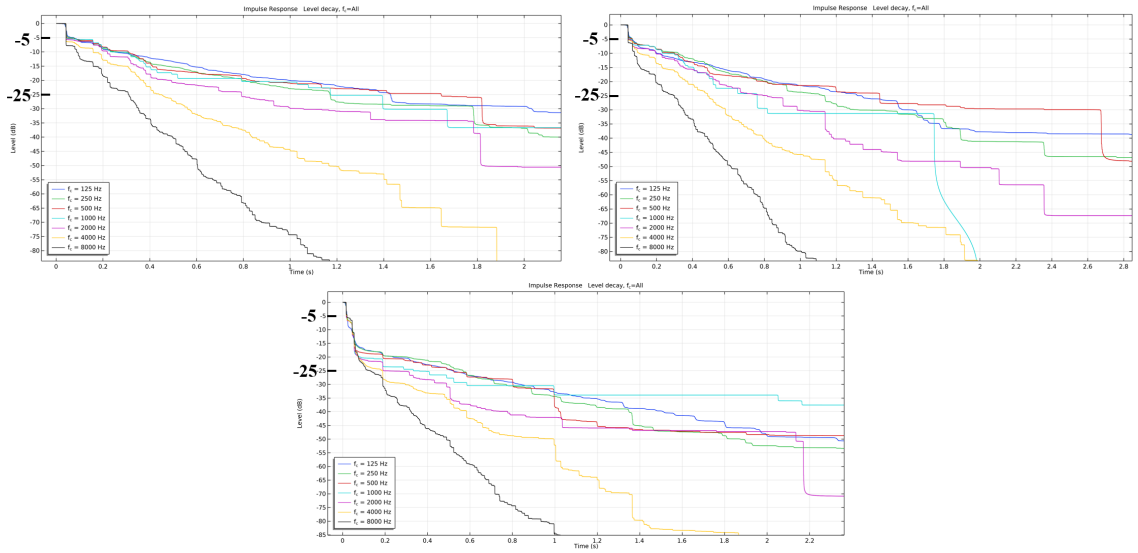

Figure 4.21: Decay curves as computed at receiver 1 (top left), receiver 2 (top right) and receiver 3 (bottom) for the seven octave bands used in the model with the source at position 3.

The corresponding reverberation times are illustrated in Figure 4.22. Highest T_{20} values are obtained by receiver 1 at 1.5 m over the ice. It shows a peak that almost reaches 5 s in the 500 Hz band. A similar peak is found in the receiver 2 results, but approximately 1 s lower. In general T_{20} results from the 3 m receiver show a similar tendency with receiver 1 results, but with slightly lower values. The results converge above 2 kHz, where no height dependency is present. The audience receiver produces much lower T_{20} values. No peak is detectable and T_{20} is pretty constant around 1.5 s until 1 kHz and falling further to 0.5 s at high frequencies.

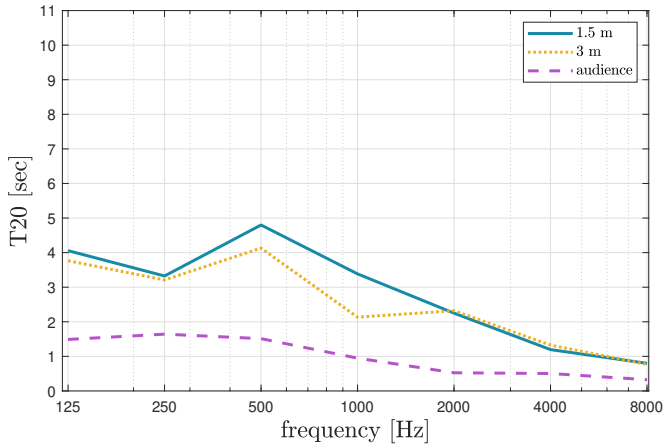

Figure 4.22: Simulated T_{20} with the sound source placed in the audience. Each line represents one receiver. Receivers 1 and 2 are located inside the rink at 1.5 m and 3 m (solid and dotted line respectively), while receiver 3 is in the audience (dashed line).

4.3.2.3 Graded temperature case without protective glass

The final model presents the case with graded temperature and ice inside the rink, however with no protective glass walls. The rink is surrounded only with the one-meter high wooden board. This case is easier to compute and could yield results in source position 1, because the ice rink wall height is significantly reduced, thus reducing the amount of produced reflections. Reverberation time results for source position 1 can be viewed in Figure 4.23. T_{20} is very low in this case. It is fairly constant with no peak, spanning between 2 s and 2.5 s among the receiver positions. At high frequencies it falls further to 1 s. The dip in receiver 2 and 3 results at 1 kHz is questionable and it is believed that it doesn't represent reality. In any case, no significant height dependency is observed in the results.

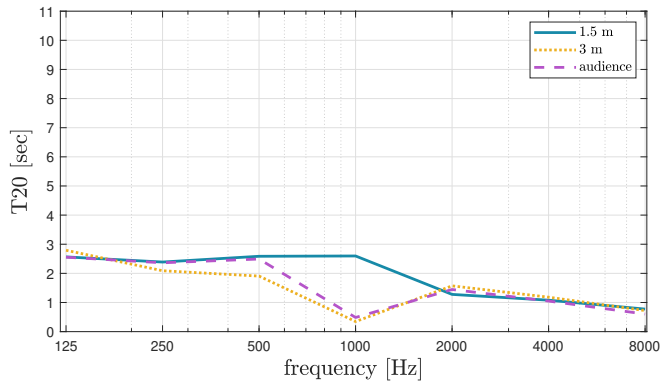

Figure 4.23: Simulated T_{20} with the sound source placed inside the rink. Each line represents one receiver. Receivers 1 and 2 are located inside the rink at 1.5 m and 3 m (solid and dotted line respectively), while receiver 3 is in the audience (dashed line).

5
Discussion

Measurement results

The new measurements in ice hall 1 support the previously performed ones, where the phenomenon of long reverberation time was initially observed. The measurements in the two additional halls prove that this is not a single hall phenomenon, since the reverberation time curves show similar tendencies in all cases. It could then be assumed that analogous T_{20} results can be expected in all ice hockey halls. Certainly deviations are to be expected, since reverberation time depends on hall properties like size, geometry and absorption among others. Deviations are to be expected even in the same hall depending on time of day or time of the year, as the outside temperature plays a role in the resulting temperature gradient. However, the temperature gradient inside the ice rink and the rink dimensions and almost the same in all halls and are those that mainly affect T_{20}. Consequently, it would be reasonable to anticipate a peak of reverberation time in the low to middle frequency range inside the rink in every hall.

By comparison of the measured reverberation time of the three ice halls (Figures 3.5, 3.9 and 3.11), it can be observed that the peak of T_{20} is located in the 400 Hz or 500 Hz band, with high reverberation times measured in a wider range, spanning between 250 Hz and 630 Hz. A strong height dependency is present in the results within this frequency range, with higher T_{20} measured at lower points inside the ice rink. Outside this range, the reverberation time is rather constant and the results don't seem to be affected by the receiver's height. In all cases much higher T_{20} values are measured when the sound source is located inside the ice rink. Depending on the hall, the peak of T_{20} can reach a value of 7 s up to 10 s when measured by the lowest receiver, located at 1.5 m above the ice surface. Lower reverberation time is obtained when the source is in the audience, with the peak being reduced by 2 s to 3 s at all receiver positions. It also tends to flatten or even disappear at higher microphone placements giving its place to a less varied curve. It should also be mentioned that at frequencies above 2 kHz there is a much stronger agreement in the results of all halls. A similar descending pattern is noticeable at all source and receiver positions, with T_{20} starting with a value of 2.5 s and decaying gradually with frequency, landing at almost 1.5 s at 10 kHz. This is due to the fact that at higher frequencies, the wavelengths of the emitted sound are so short that are mainly affected by air absorption, which is very similar in all three halls.

2D model

The 2D Axisymmetric model results come to confirm the initial hypothesis of refraction effects having an impact on the ray paths in the hall. As shown in Figure 4.4, in the graded temperature case, temperature inversion leads to downward bending of the sound rays, in contrast to the straight rays that are visible in the constant temperature case. The ray distribution throughout the space is accordingly affected, with many of the rays being trapped inside the ice rink when ice is present. They remain closer to the ice and keep being reflected on the protective glass walls, leading to a higher accumulation of energy inside the rink area. The 2D model proves that the temperature gradient and the hall geometry are sufficient for refraction to take place and have an impact on the ray trajectories and can be successfully simulated. It thus gives the green light for further investigation and evaluation of reverberation time in 3D.

3D models with constant temperature

At the beginning, a model with completely parallel rink walls was created. However, the results were not as expected, since reverberation time as shown in Figure 4.16 reaches up to 7 s instead of 3 s that was the corresponding measurement result. Parallel walls enable the formation of standing waves inside the rink. The sound rays are being reflected back and forth and since the walls are flat and of low absorption, there are no big energy losses after each reflection. Consequently, a large amount of energy remains in the rink, leading to the observed high reverberation time. A new rink geometry was then created, where the protective glass walls were slightly tilted in an attempt to reduce the amount of standing waves.

T_{20} results from the tilted wall configuration as illustrated in Figure 4.20 are much lower, around 3 s. Both source positions yield similar results. The receiver position doesn't seem to greatly affect the resulting T_{20} either. Therefore, it can assumed that reverberation time is rather constant throughout the hall. Figure 5.1 presents the previously shown 3D model results for the constant temperature case with tilted rink walls together with the corresponding results from former measurements as were presented in the Introduction. The sound source and receivers are located inside the rink. In the simulation results, T_{20} from the audience receiver is also included. The simulation results bear a big resemblance with the measured ones. The measurements show a reverberation time of about 3 s in the middle frequency range that drops to 1 s at high frequencies. The simulated reverberation time is approximately 0.5 s higher at low to middle frequencies, but follows a very similar trend in general. In both cases there is no observed difference between the receivers placed inside the rink area. It can be concluded that this tilted wall configuration is a closer representation of the real case, as in reality it is very rare to come across completely parallel walls. Moreover, the overall model can be considered to be adequately constructed. The simplified geometry and the absorption and scattering coefficients used can be considered sufficient and representative of the actual hall and the hall materials and yield reasonable results.

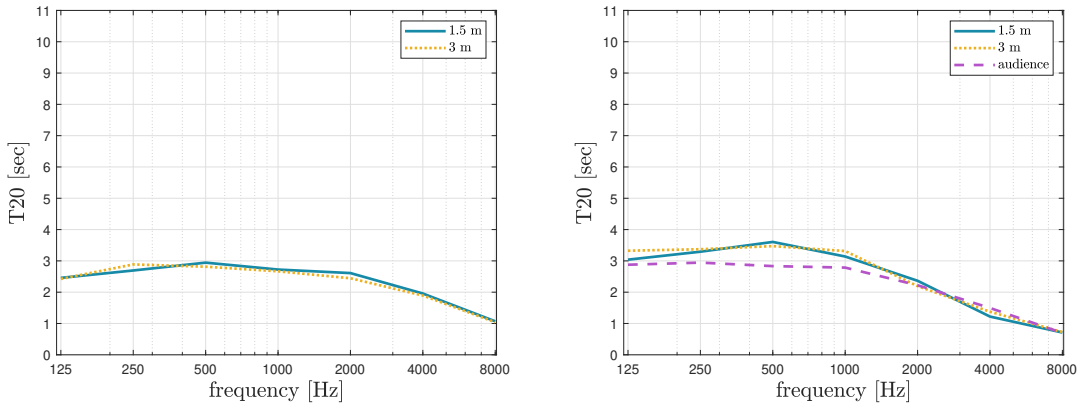

Figure 5.1: Measured (left) and simulated (right) T_{20} at various receiver positions for the case of concrete on the ground inside the rink and constant hall temperature (17 °C).

3D model with graded temperature

As explained in the Simulations chapter, the intensity computation in a graded medium is much more demanding than in a homogeneous one, as the air medium is taken into consideration and bended wavefronts are created. Moreover, for this hall size and temperature gradient, a high amount of rays is needed in order to yield reasonable reverberation time results. The computation is more tedious when the source is placed inside the ice rink. A higher amount of reflections is produced and the solver needs to take very small time steps for them to be successfully represented. For all these reasons, reasonable results could not be obtained with source position 1 since the memory requirements were too high. 260000 rays were used, which correspond to a receiver radius of 0.6 m, according to Equation 2.23. A smaller amount of rays and by extension a wider receiver radius would reduce the size of memory needed. However, the resulting reverberation time would not be representative as the receiver radius would be too wide to take into account the temperature gradient effects.

Source position 3 is less demanding, since the source is placed in the audience area and less reflections take place in the immediate vicinity of the release. Furthermore, the source is located higher and the temperature gradient is less extreme at that point. There is definitely an amount of rays that are trapped inside the ice rink and reflected as in the source position 1 case. However it is a much smaller number and the ray power is reduced by that time, so the time they remain inside the ice rink until the computation is terminated is also reduced. Consequently, it was possible to acquire reasonable results with this source position. Computed T_{20} is shown in Figure 5.2 together with the measurement results for this source placement. The reader is reminded to ignore the large peak of the measured results in the 630 Hz band (left graph), since it represents an unfortunate double shot of the start pistol and is irrelevant to the actual reverberation time. There seems to be a strong resemblance in the simulation and measurement results from receiver 1 and 2, which were

located at 1.5 m and 3 m above the ice surface respectively. A height dependency is clearly visible in both cases with higher T_{20} observed closer to the ice surface. T_{20} results from the audience receiver in the simulation are much lower than in the measurement. This could be attributed to the fact that the decay curves at this position (as seen in the bottom graph of Figure 4.21) are made up of two different slopes, with the first steeper one extending to a level as low as −20 dB in some octave bands. As a result, this slope is mostly used in the T_{20} evaluation, leading to much lower values.

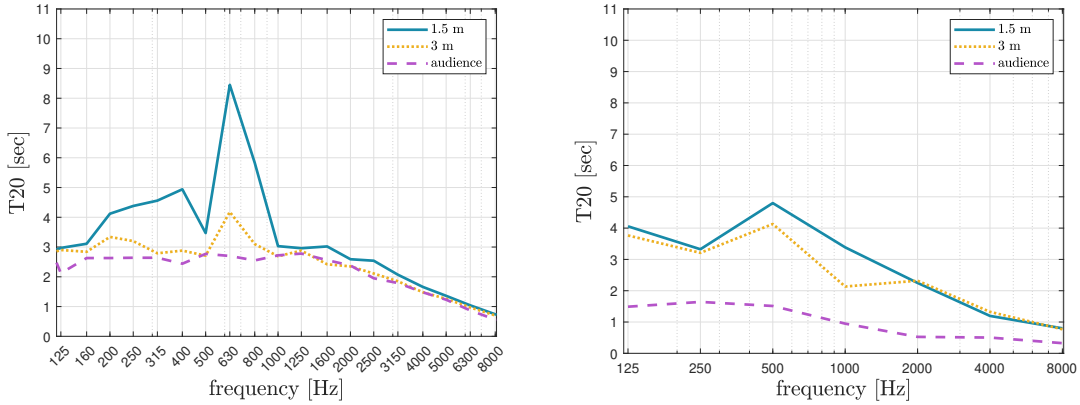

Figure 5.2: Measured (left) and simulated (right) T_{20} for the graded temperature case with the source at position 3 in the audience.

Possible 3D model improvements

The simulation results seem to bare an adequate resemblance to the measurements, therefore the COMSOL models can be considered sufficient to confirm the initial hypothesis. However, there is certainly room for further adjustments for the results to be an accurate representation of reality. A question that could be raised is whether Equation 2.23 that was used to determine the required amount of rays depending on receiver radius is also valid in the graded temperature scenario. In any case, a smaller receiver radius and therefore a larger amount of rays is assumed to increase the resolution of the produced decay curves and contribute to more reliable and accurate reverberation time results. The mesh resolution and the selected time-steps could be further studied and optimized as well. As far as the geometry is concerned, it could be modified to include some more details like door openings. Frequency-dependent scattering coefficients could be used in case there is available data in the future. Also angle-dependent absorption coefficients could be more precise in the graded temperature case.

General remarks

After having reviewed the results from both constant and graded temperature models, a noteworthy observation would be that the initial model with the parallel rink walls and the graded temperature model share lots of common features. In both

cases a larger amount of energy is trapped inside the rink. In the constant temperature case, this can be attributed to the rink wall shape that creates standing waves. In the graded temperature case, refraction keeps the sound rays closer to the ground, as previously explained. This larger amount of energy leads to increased reverberation time in the rink. Figure 5.3 presents again the results from the first measurement together with the simulation results of the constant case with parallel walls with the source in position 1. What is interesting is the fact that in both cases the highest values of T_{20} are located in similar frequencies. Of course the measurement results are more detailed since they are presented in third octave bands, but in general the tendency is the same. Moreover, there is a clear dependency of the results on receiver height.

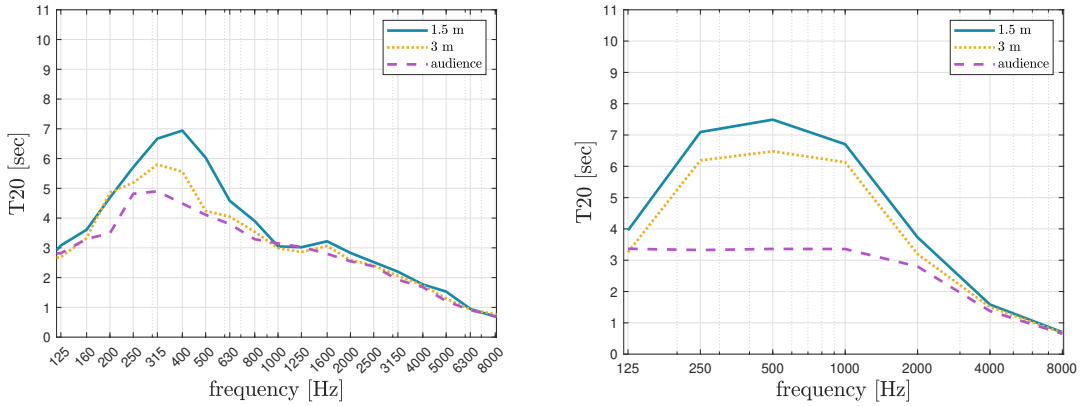

Figure 5.3: T_{20} results from the first measurement (left) and from the simulation of the constant temperature case with parallel rink walls (right).

In either case, this energy concentration inside the rink hinders the creation of a diffuse field in the hall, thus leading to coupled room effects. As a result, double-sloped decay curves are created. As mentioned in the Theory, this means that the various modes of the room are decaying with different damping constants. Double-sloped decay curves can be seen in Figure 4.15 for the constant temperature, parallel-wall case and Figure 4.21 for the graded temperature case at all receiver positions. The coupled-room assumption is also confirmed by the measurement results, as shown in Figures 3.6 and 3.7. The fact that T_{30} is longer than T_{20} in some frequencies points out that they are calculated from two different slopes. It can be concluded that the set of modes corresponding to those frequencies are the ones that are less damped and decay with a lower rate. A question then would be why this set of modes in particular. It could be attributed to their wavelength. Lower frequencies have larger wavelengths that can pass through the walls, while higher frequencies with shorter wavelengths are primarily affected by air absorption. That means that the middle frequencies are those whose wavelengths fit to the dimensions of the ice rink and are perpetually reflected.

6
Conclusion

The aim of this thesis was to study and explain the high reverberation time that was observed at certain frequency bands after measurements in an ice hockey hall. The measurements were repeated and extended to two more halls and thus verified that this is a phenomenon concerning ice hockey halls in general. Through simulations in COMSOL Multiphysics® it was shown that the temperature gradient and ice rink dimensions are sufficiently large for refraction effects to take place. Moreover, the simulated reverberation time results came close to the measured ones, proving that the predescribed phenomenon can be modelled. It was concluded that the reason why longer reverberation is present in the low to middle frequency range is a combination of factors. Sound rays are bended downwards due to refraction and then they are being trapped inside the protective glass walls that surround the ice rink. Since there is very little absorption, they are being reflected back and forth leading to an increased amount of energy in the rink. The frequency range in which this phenomenon is detected corresponds to the modes that fit the rink dimensions, which consequently dominate the reverberation time.

A model without protective glass walls was constructed to showcase the effects of added absorption on the reverberation time. T_{20} was then significantly decreased and remained constant throughout the frequency range. It was thus proved that with added absorption, the amount of reflections would be effectively reduced, contributing to much shorter reverberation time. In reality, however, it is difficult to apply absorption inside the rink. The protective glass walls are serving specific functions, supporting the sport and audience safety and are constructed according to strict rules. One suggestion to reduce the amount of reflections in the rink could be to slightly tilt all walls upwards so that the sound rays are directed upwards and escape the rink. Another suggestion would be to use perforated glass in order to add some absorption on the walls. The amount of perforation should be such that will not obstruct visibility and the glass should be strong enough to hold the force of the players and the puck. These are some ideas for future consideration. It remains to be seen whether they can be successfully implemented or other possible improvements can be explored. By present, it would be advised that the players should wear some kind of ear protection if it doesn't obstruct their performance, so they are shielded from high noise level exposure.

References

[1] Leo Beranek. *Concert Halls and Opera Houses: music, acoustics, and architecture*. New York, NY: Springer New York, 2004. ISBN: 978-1-4419-3038-5. DOI: 10.1007/978-0-387-21636-2.

[2] Michael Barron. *Auditorium Acoustics and Architectural Design*. Second Edition. Taylor & Francis e-Library, 2009.

[3] Heinrich Kuttruff. *Room Acoustics*. Sixth edition. | Boca Raton : CRC Press, [2017]: CRC Press, Oct. 2016. ISBN: 9781315372150. DOI: 10.1201/9781315372150.

[4] Mendel Kleiner. *Acoustics and audio technology*. J. Ross Pub, 2012. ISBN: 9781604270525.

[5] Allan D. Pierce. *Acoustics: An Introduction to Its Physical Principles and Applications*. Third Edition. Cham: Springer International Publishing, 2019. DOI: 10.1007/978-3-030-11214-1{_}1.

[6] Michael Vorländer. *Auralization - Fundamentals of Acoustics, Modelling, Simulation, Algorithms and Acoustic Virtual Reality*. Berlin, Heidelberg: Springer Berlin Heidelberg, 2008. ISBN: 978-3-540-48829-3. DOI: 10.1007/978-3-540-48830-9.

[7] International Organization for Standardization. *Acoustics - Attenuation of sound during propagation outdoors - Part 1: Calculation of the absorption of sound by the atmosphere (ISO 9613-1)*. 1993.

[8] Trevor J. Cox and Peter D' Antonio. *Acoustic Absorbers and Diffusers: Theory, design and application*. Spon Press, 2004.

[9] COMSOL AB. *Acoustics Module User's Guide, COMSOL Multiphysics® v. 6.1*. Stockholm, Sweden, 2022.

[10] International Organization for Standardization. *Acoustics - Measurement of room acoustic parameters - Part 1: Performance spaces (ISO 3382-1)*. 2009.

[11] Norsonic AS. *Nor140 Instruction Manual - Instrument Software 4.0*. 2017.

A
Appendix

Table A.1: Frequency-dependent absorption coefficients α of the ice hall materials used in the simulation.

Material	Absorption coefficient						
	125 Hz	**250 Hz**	**500 Hz**	**1 kHz**	**2 kHz**	**4 kHz**	**8 kHz**
Ice	0.02	0.02	0.02	0.02	0.02	0.02	0.02
Concrete	0.10	0.05	0.06	0.07	0.09	0.08	0.08
Glass	0.18	0.06	0.04	0.03	0.02	0.02	0.02
Board	0.42	0.21	0.10	0.08	0.06	0.06	0.06
Seating	0.44	0.60	0.77	0.89	0.82	0.70	0.80
Plaster walls	0.15	0.10	0.06	0.04	0.04	0.04	0.05
Paroc walls	0.10	0.20	0.10	0.10	0.05	0.05	0.05
Curtain	0.15	0.10	0.06	0.04	0.04	0.04	0.05
Ceiling	0.68	0.81	0.93	1.00	0.95	0.84	0.75

Table A.2: Scattering coefficients s of the ice hall materials used in the simulation.

Material	Scattering coefficient
Ice	0.05
Concrete	0.05
Glass	0.05
Board	0.05
Seating	0.30
Plaster walls	0.05
Paroc walls	0.05
Curtain	0.05
Ceiling	0.20

DEPARTMENT OF SOME SUBJECT OR TECHNOLOGY
CHALMERS UNIVERSITY OF TECHNOLOGY
Gothenburg, Sweden
www.chalmers.se

CHALMERS
UNIVERSITY OF TECHNOLOGY